Geological Interpretation of the Reservoir and Pay Distribution of the G3.2 and G5.2 series of the Shwe Field, Myanmar*

Robert C. Shoup[1], Allan J. Filipov[2], and Mike Hiner[3]

Search and Discovery Article #20401 (2017)**
Posted October 2, 2017

*Adapted from extended abstract prepared in conjunction with oral presentation given at 2017 Third AAPG/EAGE/MGS Oil and Gas Conference, Yangon, Myanmar, February 22-24, 2017

[1]Subsurface Consultants & Associates, Houston, TX, United States (rcs@clasticman.com)
[2]EMGS, Kuala Lumpur, Malaysia
[3]Consultant, Houston, TX, United States

Abstract

The Shwe, Shwe Phyu, and Mya gas fields were discovered between 2004 and 2006 by Daewoo International in Blocks A-1 and A-3 offshore Myanmar. Daewoo drilled the Shwe 1, the first gas discovery after the vertical Shwe 1 well was found to be devoid of reservoir. Subsequent to the discovery of the Shwe Field, Daewoo drilled the Shwe Phyu gas discovery north of Shwe in 2005 and the Mya gas discovery south of Shwe in 2006. Pay sands in the Shwe Field occur in two reservoir series, the G5.2 and the G3.2. The lower G5.2 reservoir series is characterized by multiple stacked lobe elements consisting of amalgamated and layered sheet sandstones. In contrast, the upper G3.2 reservoir series consists of channel and overbank deposits, which are characterized by thin-bedded sandstones with low net-to- gross ratio as well as low-resistivity pays. The distribution of reservoirs and pays across the Shwe Field is complicated as pay sands are commonly juxtaposed against wet sands. Various models have been proposed to explain the complexities observed in the reservoir connectivity and in the distribution of gas bearing versus wet reservoirs. Kim et al. (2012) use a depositionally simple mode in which the G5.2 reservoirs were deposited in multiple lobes and the G3.2 reservoirs were deposited in multiple channel levee complexes. Other authors call on a more complex model of interbedded lobes, channels, and slumps sourced from both the northwest and the northeast whereas others invoke an even more complex model with several reservoirs consisting of injectites.

Introduction

The Shwe, Shwe Phyu, and Mya gas fields were discovered between 2004 and 2006 by Daewoo International in blocks A-1 and A-3 offshore Myanmar (Yi, et al, 2015). Daewoo drilled the Shwe 1st gas discovery after the vertical Shwe 1 well was found to be devoid of reservoir. Following the discovery of the Shwe Field, Daewoo drilled the Shwe Phyu gas discovery north of Shwe (2005) and the Mya gas discovery south of Shwe in 2006 (Figure 1). This paper focuses only on the Shwe Field. The gas encountered in the Shwe Field is biogenic in origin and

recoverable reserves for the Shwe Field are reported to range from 2.87 to 4.67 TCF. Recoverable reserves have been reported for the Shwe Phyu field to range from 0.38 – 0.91 TCF and 1.28 – 2.16 TCF for the Mya Field. (Kim et al, 2012).

Pay sands in the Shwe Field occur in two principal reservoir series at 2900-3100m below the mud line, the G5.2 and the G3.2. The G5.2 reservoir series is characterized by multiple stacked lobe elements consisting of amalgamated and layered sheet sandstones. In contrast, the upper G3.2 reservoir series consists of channel and overbank deposits, which are characterized by thinly bedded sandstones with low net-to-gross ratio (avg. 33%; Yang and Kim, 2014). Thinly bedded gas-bearing reservoirs are common in this depositional setting, and can contribute significant volumes of recoverable reserves to a field yet they are not easily recognized using conventional well logging tools which cannot resolve the contrast between the shale and the sand resistivity. These thin-bedded sections appear as "low-resistivity pay" zones and a vertical resistivity measurement, core and borehole imaging are often used to detect, delineate and analyse the section for potential pay.

The distribution of reservoir and pay sands across the Shwe Field is complicated and pay sands are commonly juxtaposed against wet sands. Various models have been proposed to explain the observed complexities in reservoir connectivity and the distribution of gas bearing versus wet reservoirs. Kim et al (2012) use a simple depositional model in which the G5.2 reservoirs were deposited in multiple lobes whilst the G3.2 reservoirs are interpreted as being deposited in multiple channel levee complexes. Later authors propose a more complex model of interbedded lobes, channels, and slumps sourced from both the northwest and the northeast (Yang et al, 2015) while others invoke an even more complex model involving several reservoirs consisting of injectites (Cossey et al, 2013, Yang and Kim, 2014).

This paper uses multiple geologic cross sections to evaluate which of these depositional models best explains the distribution of reservoirs and the distribution of pay sands versus wet sands.

Data

The data for this study comes from various publications (Kim et al. 2012, Cossey at el, 2013, Yang and Kim, 2014, Yang et al, 2015) and includes seismic amplitude extractions for the G3.2 and the G5.2 reservoirs, core photos for the G3.2 and the G5.2 reservoirs, portions of ten wells, and five seismic lines.

Regional Setting

The Shwe Field is located in the Rakhine Basin offshore northwestern Myanmar in Blocks A1 and A3 (Figure 1) near the shelf-slope break, in 100 meters of water. The Shwe, Shwe Phyu, and Mya Fields consist of Pliocene aged turbidites sands deposited (Carter, 2015, Cliff and Carter, 2016) along the slope and toe of slope. The principal source of sediments is the Bengal Fan to the north – northwest of the Shwe Field (Figure 2). Uplift of the Indo-Burma Range and mass wasting of the shelf to the east of the Shwe Field may have provided a secondary source for sediments (Andy Racey, Personal Communication).

The Rakhine Shelf comprises an Eocene to Recent aged accretionary prism formed by subduction of the Indian Plate beneath the Sunda Plate (Carter, 2015, Cliff and Carter, 2016). West-verging thrust faults form a series of northwest to southeast striking fault propagation folds

(Figure 3). The Shwe Field is located between the Shwe and Ngwe anticlines (Yang and Kim, 2014), where the reservoirs are found on the western flank and crest of the Shwe Anticline (Figure 4). The northwest-southeast oriented strike line, parallel to the main depositional direction (Yang and Kim, 2013) indicates the Shwe Phyu, Shwe, and Mya reservoirs were deposited near the transition from the slope to the toe of slope (Figure 4).

Deepwater Depositional Systems

When interpreting geological cross-sections it is important to have a thorough understanding of the facies distribution of the depositional systems in order to make reasonable and valid correlations between wells. Prior to examining the cross sections, the facies types and their distribution within deepwater depositional systems will be discussed.

There are considerable differences in the reservoir distribution and connectivity between turbidites deposited on the slope and the toe of slope. Type A turbidites (Dattilo, 2013) are deposited on an unrestricted slope (Figure 5) and are associated with the bypass facies of the fan system. Since there is little to no change in gradient across the slope, turbidity flows are unconfined and continuously transport sediments from the shelf to the toe of the slope (Prather, 2003, Beaubouef, 2004, Sawyer, et al, 2007, Kneller, 2012, Dattilo, 2013, Kneller et al, 2016). Unconstrained slope deposits are characterised by channel-levees, crevasse splays, and occasional submarine canyons or gorges. The channel systems deposited on the slope typically show a meandering geomorphology (Figure 6), with the degree of sinuosity controlled principally by the dip of the slope (Lazarus and Constantine, 2013). Since unconstrained slope turbidite deposits typically consist of multiple laterally amalgamated meandering channel-levee complexes (Clemenceau, 2000, Sawyer et al, 2007, Cross et al, 2009) the associated reservoirs are not laterally extensive, particularly along depositional strike.

Once the turbidity flow reaches the toe of slope it loses velocity and eventually settles out in a lobate pattern (Figure 7). As each lobe builds up the gradient, subsequent turbidity flows will avulse toward the lower gradient, resulting in the deposition of multiple stacked fan lobes. Lobes sourced from multiple channels may coalesce to form a fan apron (Figure 7, Prather, 2016). These lobes can extend across the area of the fan to form laterally extensive reservoirs.

There are four elements with the potential to be reservoir bearing in turbidite depositional systems: fan lobes, bypass channel – levee complexes, gorges, and slumps or debris flows (Figure 8).

Bypass channel - levee complexes are defined as type A turbidites (Dattilo, 2013) deposited on the slope and the transition from slope to toe of slope and consist primarily of thick marine and slope shales and occasional sand-filled channels. Channels are typically easy to recognize on seismic, as they tend to have a high acoustic impedance contrast and exhibit a seismic amplitude anomaly. The channel system is elongate in a dip direction, typically meandering in nature and may have associated point bar and crevasse splay deposits. Localized slumps form on the edges of the channels as the channel erodes into the slope (Sawyer et al, 2007).

Fan lobes are deposited on the basin floor (Type C, Dattilo, 2013) or in ponded basins (Type B, Dattilo, 2013). Although the overall sequence coarsens upward, the individual beds are graded and fine upward. Individual sandstone beds of the lobes are separated by slope and marine

shale. In the lower fan the intervening shale beds are generally thicker than the sandstone beds whereas in the upper fan the sandstone beds are generally thicker than the shale beds. Lobes in the middle to upper fan may have multiple distributary channel levee complexes (Figure 8) with the number of channels increasing in a proximal direction. These channels are typically in communication with the lobes. Individual beds in the lobes will be continuous across the fan with few inherent lateral flow barriers. For large fan systems, this extensive lateral connectivity can provide strong aquifer support. In smaller lobes, the aquifer support may be minimal.

Turbidity flows are initially deposited as unconsolidated beds with very high water content. If these beds are disturbed by tectonic activity or are loaded by a subsequent turbidite before the bed has consolidated, then the bed can rapidly de-water creating soft-sediment deformation structures (Figure 9). This soft sediment deformation is typically confined to a single bed and can form a lateral flow baffle for that bed.

Gorges are seaward extensions of a submarine canyon and are analogous to incised valley systems. They are incised into the section and typically exhibit a meandering pattern inherited from the original channel. Incised valleys can range in thickness from 50 meters to over 1500 meters. Gorge fill-sequences consisting of multiple amalgamated channel sands and interbedded shales can exhibit a wide range of net to gross ratios that can be as high as 90%. Small scale slumping along the margins widens the gorge during incision (Shipp et al, 2000) such that the edges and base of a gorge tend to act as a fluid migration barrier, preventing or inhibiting communication between the gorge-fill sequence and the incised sequence.

Debris flows and mass transport deposits are common in deepwater depositional settings are triggered by tectonic events or major storms. They are commonly tens to hundreds of square kilometres in extent and typically extend from the shelf-edge or upper slope to the abyssal plain (Figure 10). They can be recognized on seismic by their chaotic seismic appearance (Figure 8). Debris flows are large-scale gravity slide phenomena formed by slope failure, which causes material to move en masse as a non-Newtonian fluid with laminar flow (Houghton et al, 2006, Kneller, 2012). Debris flows consist of an updip extensional area, a translational middle, and a downdip compressional toe (Figure 10, left). Although mass transport deposits and debris flows may contain reservoirs, they more typically remove reservoirs from the updip extensional head and destroy depositional connectivity and permeability in the translational middle. In the compressional toe, beds are highly discontinuous (Figure 10, middle). Debris flows, therefore, commonly serve as a barrier to fluid migration rather than as a reservoir.

Slumps are small-scale gravity slide events, which typically extend over an area of a few square kilometres or less. They can be found anywhere within the deepwater depositional system. Slumps are U-shaped features (Figure 10, right) that scour out material in the extensional head and translate that material to the compressional toe. As with debris flows, slumps typically remove reservoirs or destroy depositional connectivity and permeability.

Core

Two core photos from well Shwe 2A were published by Yang and Kim (2014). The first core is from the G3.2 reservoir series (left, Figure 11) and the second core is from the G5.2 reservoirs (right, Figure 11). In the core of the G3.2 series, several thin sands and interbedded shales may represent lower fan lobes or levee and crevasse splay deposits characteristic of a bypass sequence. Yang and Kim (2014) interpreted these sands as being proximal overbank deposits, dominated by a mud stone interval, with interbedded, parallel-stratified and ripple laminated

sandstone characteristic of a channel levee complex. The core of the G5.2 series is characteristic of sandy fan lobes. The thickness of the sand (Figure 11) suggests proximal deposition in the mid to upper fan. Yang and Kim (2014) interpreted these sands as representing amalgamated sheet sands typical of a fan lobe.

Cross Sections

Four cross sections were constructed for this study (Figure 12) consisting of two strike sections parallel to the Shwe anticline (cross sections 1 and 2) and two dip sections extending from the flank to the crest of the Shwe anticline (cross sections 3 and 4). Interpreting multiple cross sections ensures that the correlation of the various reservoir sands is consistent and loop-tied. This means that the distribution of the hydrocarbons is both consistent and possible; that no wet sands are structurally high to correlative pay sands and, that the final correlations are consistent with the seismic data. All cross sections were constructed on both a structural datum (sea level) and a stratigraphic datum (top G3.2). This iteration between structural and stratigraphic cross sections is a powerful tool in helping to generate consistent and valid correlations. The uppermost cross section shown in Figure 13, Figure 14, Figure 15 and Figure 16 is the stratigraphic cross section. The lower cross section is the structural cross section. It should be noted that the published versions of the wells available do not allow detailed correlations and the interpretations shown in Figure 13, Figure 14, Figure 15 and Figure 16 are, by necessity, more stylistic.

Cross section 1 is a strike cross section extending along the flank of the Shwe anticline from well Shwe 2A in the north through wells Shwe 3 and 6 to well Shwe 4 in the south (Figure 13). The upper section is a stratigraphic section hung on the G3.2 datum (Figure 13A) and the middle section is as structural section with a sea level datum (Figure 13B). The seismic line along the line of the cross section (Figure 13C) was published in Cossey et al (2013). Three distinct correlative lobes are interpreted for the G5.2 series on this cross section. The oldest observed lobe, G5.2A, is interpreted to pinch-out to the south. Lobe G5.2B pinches-out to the north, and Lobe G5.2C, which is gas bearing, extends across the entire cross section. What appears to be a gas water contact for this lobe can be seen in well Shwe 6.

The thick pay sand seen at ~3200 m in well Shwe 3 is not a G5.2 lobe, but a gorge of G3.2 age that has cut down through the G5.2B lobe. The entire thick sand in the Shwe 3 well has been interpreted as the G3.2A gorge-fill sequence with the lower-most portion of the gorge-fill sand being wet (Figure 13). Alternatively, the base of the gorge could be interpreted as the base of the gas pay. If this latter interpretation is correct, then the wet sands at the base of the thick sand sequence seen in the well would be sands of either the G5.2A or G5.2B lobes. It was not possible to correlate any G3.2 series sands from well to well in a manner that is consistent with the interpretation of the other cross sections. This suggests that they represent bypass channel-levee deposits; which fits with the interpretation of the core data. The channels in the southern part of the cross section are wet, whereas those in the central and north portion of the section are mostly gas bearing.

A thin chaotic seismic facies can be seen just below the G3.2 (green event, Figure 13) and above the G5.2 (blue event, Figure 13). This could be interpreted as a mass-transport deposit resulting from a shelf collapse to the east. A highly chaotic seismic facies seen below the Pliocene sequence boundary (red event, Figure 13) has the appearance of a large debris flow deposit demonstrating that debris flows are present near the Shwe Field. However, it is not possible with the available data to confirm the presence of the debris flow and consequently it has not been shown on the cross section interpretations. A large slump feature can be seen on the southern end of the seismic line (Figure 13) which appears to cut down through the G3.2 and G5.2 series and the Pliocene sequence boundary (red event, Figure 13).

Cross section 2 is a strike cross section extending along the crest of the Shwe anticline from well Shwe 2A in the north through wells Shwe 5 and 5A to wells Shwe 1A and 1 in the south (Figure 14). The seismic profile along the line of the cross section was published in Cossey (2013). Four correlative lobes are interpreted for the G5.2 series. Lobe G5.2A and G5.2C are interpreted to pinch-out to the south while lobes G5.2B and G5.2D pinch-out to the north. Lobe 5.2C is seen in Well Shwe 2 to be pay bearing. This lobe is structurally low to wet G5.2 lobes observed in wells Shwe 5, 5A, and 1. There is seismic evidence that a gorge cuts down into the uppermost G5.2 lobes between wells Shwe 2A and Shwe 5A (Figure 14C). It is not possible with the available data to determine if this is the same gorge observed in well Shwe 3 (Figure 13 and Figure 15). The gorge seen on the seismic profile (Figure 14) may trap the gas in lobe G5.2C, preventing it from migrating to the crest although it is considered more likely that lobe G5.2C pinches out between wells Shwe 2A and Shwe 5 such that the gas is stratigraphically trapped.

Multiple G3.2 series channel sands are interpreted on cross section 2 (Figure 14). As with cross section 1 (Figure 13), it is not possible to make consistent well-to-well correlations of any G3.2 series sands. Most of the channels are pay bearing although several wet channels are observed in wells Shwe 5 and 5A. A thin chaotic seismic facies can be seen just below the G3.2 event (green) between wells Shwe 5 and Shwe 1A on the seismic profile for cross section 2 (Figure 14C). This could be evidence for the presence of a mass-transport deposit in the lower G3.2 series as described for cross section 1 (Figure 13). A slump feature seen in well Shwe 1 erodes and removes the G3.2 series reservoirs seen in well Shwe 1A as well as the G5.2D lobe. This is likely to be the same slump observed on the seismic line associated with cross section 1 (Figure 13).

Cross section 3 is a dip cross section extending from the flank to the crest of the Shwe anticline from well Shwe 3 in the southwest through well Shwe 5A to well Shwe 5 in the northeast (Figure 15). This cross section loop ties cross sections 1 and 2. A corresponding seismic section along the line of the cross section was published by Yang and Kim (2014). Three correlative lobes have been interpreted for the G5.2 series on this cross section. Lobe G5.2A is observed in well Shwe 3 and is inferred to pass below wells Shwe 5 and 5A. The G5.2 lobes B and D are observed in wells Shwe 5 and 5A, but were erosively removed by the G3.2A gorge (Well Shwe 3, Figure 15).

As seen on cross section 1 (Figure 13), the thick pay sand seen at ~3200 m in well Shwe 3 is not a lobe, but a gorge of G3.2 age. Multiple G3.2 series channel sands are interpreted on this cross section. As with the strike cross sections, it was not possible to definitively correlate any G3.2 series sands from well to well. A second gorge is seen on the seismic to the southwest of well Shwe 3 (blue, Figure 15). This gorge is younger than G3.2 and can be seen cutting down into the G5.2 section and potentially through the G5.2C lobe as well.

Cross section 4 is a dip cross section extending from the flank to the crest of the Shwe anticline from well Shwe 6 in the southwest through well Shwe 1A to well Shwe 1 in the northeast (Figure 16), loop tying cross sections 1 and 2. No seismic profile was available along the line of this cross section. All four G5.2 lobes interpreted on cross sections 1 to 3 (Figure 13, Figure 14, Figure 15) can be observed on this cross section as is the gas water contact for lobe G5.2C seen in the Shwe 6 well. The structurally high G3.2 channels on this section are gas bearing whereas the structurally low G3.2 channels are wet. However, as seen in Figure 14 and Figure 15, not all of the crestal channels are gas bearing.

Shwe Field Depositional Interpretation

The turbidite reservoirs of the G5.2 series are interpreted as having been deposited on the abyssal plain at the toe of slope and these reservoirs tend to be correlative in a number of wells indicating deposition in fan lobes. Correlations indicate the presence of at least four separate fan lobes sourced from the northwest and shingled in an east-west direction because of avulsion. The G5.2 A, B and D lobes are wet and the G5.2 C lobe is gas bearing. The oldest lobe is the G5.2A lobe, which was deposited on the western flank of the Shwe anticline (Figure 17A). The fan system appears to have avulsed to the east, depositing the G5.2B lobe on the crest of the Shwe anticline (Figure 17B). The G5.2C lobe avulsed back to the west. The north and western margin of the G5.2C lobe was subsequently eroded by the G3.2A gorge (Figure 17C). The youngest recognized fan lobe is the G5.2D lobe which appears to have again shifted eastward over the crest of the Shwe anticline (Figure 17D). The G3.2A reservoir is interpreted to be a submarine incised valley (gorge) that cut down into the G5.2 reservoir series (Figure 18). Although it is juxtaposed against G5.2 reservoirs, the reservoir is actually of G3.2 in age (Figure 13 and Figure 15). It is not possible to define the limits of the gorge on either the published G5.2 or G3.2 amplitude maps (Figure 18) and consequently limits of the gorge are highly inferred. The G3.2 series reservoirs are interpreted to consist of a series of channels deposited in the lower slope or near the transition from the slope to the basin floor. The available well data indicates numerous channels; however, it is not possible to define specific channels from the G3.2 seismic amplitude extraction (Figure 19). The channels are drawn schematically as a typical meander belt (Figure 19 left). Some of the channels are shown as gas-bearing pay and others are shown as wet. There is some seismic evidence for a debris flow in the lower portion of the G3.2 series (Figure 13 and Figure 14) although it is not possible to confirm the presence of a debris flow or determine its aerial extent with the available public data.

Shwe Field Hydrocarbon Distribution

Hydrocarbons of the Shwe Field consist of biogenic gas formed contemporaneously with reservoir deposition and trap formation (Das et al, 2008). Retention of the gas is the critical petroleum system element risk for the Shwe Field. Looking first at the G5.2 series reservoirs, four individual lobes have been identified of which only one is pay-bearing (G5.2C). As can be seen in cross sections 2 and 4 (Figure 14 and Figure 16), the G5.2C lobe is not the structurally highest lobe yet it is the only pay bearing lobe. We can infer that the G5.2C lobe is stratigraphically trapped to the northeast by the pinch out of the lobe. The trapping mechanism for the G5.2C lobe to the northwest is inferred to be by isolation of the lobe when it was cut by a gorge. The trapping gorge could be the G3.2A gorge but it is considered more likely to be the blue gorge seen on cross section 3 (Figure 15). The G3.2A gorge is also pay bearing, indicating a stratigraphic trapping element that prevents northwest migration of gas out of the reservoir. It is not possible with the available data to determine how, or where, the G3.2A gorge is trapped. Two possibilities can be considered; a bend in the gorge that prevents northward migration of the gas, or a second gorge system that cuts down through and traps the G3.2A gorge. The latter possibility seems most likely as we can see on cross section 3 (Figure 15) that the blue gorge does truncate the G3.2A gorge. Looking at the G3.2 series sands, some channel-levee reservoirs are gas bearing and others are wet, including channels seen near the crest of the Shwe anticline. Since these were deposited as a series of meandering channels in the bypass section, the predominant control on the distribution of gas will be the orientation of the meander loop. Meander loops that cross the structure with the 'horns' of the meander loop pointing downdip can trap migrating hydrocarbons (red channels, Figure 19). Meander loops that cross the structure with the 'horns' of the meander loop pointing updip will allow hydrocarbons to migrate updip and be lost as will channels oriented parallel to the dip direction which will not seal (yellow channels, Figure 19).

Risk Reduction

The distribution of gas-bearing and wet sands in the Shwe Field, especially with wet sands on or near the crest of the Shwe Anticline suggests that the pays are stratigraphically trapped. There are a number of potential stratigraphic traps inherent in deepwater depositional systems. Ideally, we want to be able to delineate pay sands from wet sands before drilling, especially in deep water where drilling costs are high and development options are limited. To accomplish this, we need to consider methods to help reduce risk by being able to identify pay pre-drill. There have been considerable advances in seismic acquisition, processing, and imaging over the last few years. Most of these methods, especially when combined with a thorough understanding of the depositional system, allow interpreters to define the distribution of the reservoir facies with a high degree of accuracy. However, the majority of these methods do not differentiate reservoirs that are pay-bearing from those that are wet. The traditional approach to reducing risk is to use seismic amplitude extractions, inversion, and AVO as direct hydrocarbon indicators. In the case of the Shwe Field, the application of seismic amplitudes appears to have allowed interpreters to successfully delineate the pay-bearing G5.2C lobe, but not the distribution of pay-bearing channels in the G3.2 series.

Deepwater channels, such as those observed in the G3.2 reservoir series, consist of clean, porous sandstone encased in shale that typically show up as seismic amplitude anomalies. These anomalies cannot be differentiated from hydrocarbon indicators since the response occurs over a wide range of hydrocarbon saturations. Other limitations related to acquisition geometries and the seismic processing sequences make pre-drill prediction difficult without a means to discriminate the wet or low saturation channels from hydrocarbon-bearing channels. If the reservoir resistivity can be established, the targets with higher resistivity and low impedance have a better chance of encountering hydrocarbons, though uncertainties in the volume remain.

Controlled Source Electro Magnetics or CSEM can be used to map subsurface resistivity and detect anomalous resistive bodies related to a lack of brine at that location. A resistive anomaly located in a prospect after 3D CSEM inversion can be expressed in terms of resistivity thickness and area and Monte Carlo simulations can be used to generate a probability distribution of the net saturated rock volume (Filipov et al, 2014, Baltar and Roth, 2015). Figure 20, from the Foz do Amazonas basin in Brazil, illustrates a series of slope channels (green) found using 2D seismic data (Pedersen and Hiner, 2014). The yellow highlighted areas (Figure 20, left) are channels that exhibit a strong seismic amplitude anomaly. The right side of Figure 20 clearly shows only a few of those channels exhibit anomalous resistivity. However, an integrated interpretation must be undertaken to mitigate other geological factors that create high resistivity before these channels can be interpreted as pay bearing. In addition to CSEM, evaluation of those physical seismic attributes associated with frequency attenuation and absorption can be useful in delineating hydrocarbon-bearing reservoirs, particularly those that are gas bearing. These attributes include Relative Acoustic Impedance, Instantaneous Frequency, Instantaneous Acceleration AC(t), Instantaneous Bandwidth B(t), and Instantaneous Q. An excellent summary of the various seismic attributes and their applications is found in Subrahmanyam and Rao (2008).

Spectral decomposition is another methodology that can help discriminate hydrocarbon-bearing reservoirs from wet reservoirs. Spectral decomposition transforms seismic data from the time domain to time vs. frequency domain, which can illustrate many features that are not apparent in time domain representation, including the presence of hydrocarbons (Khonde and Rastogi, 2013). When spectral decomposition is carried out on seismic data the resultant frequency slices can illuminate frequency anomalies associated with hydrocarbons. Low frequency

slices show higher amplitudes than corresponding high frequency slices at hydrocarbon zones Thus, spectral decomposition can act as a direct hydrocarbon indicator (DHI).

Figure 21 shows a seismic section from a Nigerian data set (Khonde and Rastogi, 2013). The yellow arrows indicate known hydrocarbon zones while green arrows indicate faults. The middle image is a 20 Hz frequency slice obtained after spectral decomposition in which hydrocarbon-bearing reservoirs appear as high-amplitude low frequency anomalies (red anomalies on the 20 Hz frequency slice). Most of these hydrocarbon-bearing reservoirs are not apparent on the 33 Hz frequency slice (Figure 21 right).

Given the variability of pay versus wet sands observed in the Shwe Field it would be prudent to apply multiple methods to define those sands likely to be saturated with hydrocarbons. This is especially true in deepwater settings where high drilling and development costs combined with a limited number of development options makes pre-drill determination of hydrocarbons critical. It is also critical to have a thorough knowledge of the distribution of reservoir facies within deepwater depositional systems in order to reduce risk. This knowledge, combined with the application of multiple geophysical methodologies such as CSEM, seismic attributes, and spectral decomposition can go a long way to maximizing the volume of hydrocarbons that can be recovered and minimize the number of wells needed to recover these volumes.

Conclusions

The Shwe Field data illustrates that seismic sequence stratigraphy and reservoir delineation from amplitude extractions are insufficient to fully delineate the distribution of the pay-bearing reservoir facies in turbidite systems. In addition to the seismic interpretation, the evaluation of multiple cross sections combined with a thorough knowledge of the depositional system is needed to understand the distribution of both the reservoir facies and the fluids. The correlation of four geologic cross sections across the Shwe Field indicates that the lower reservoir series, the G5.2, were deposited as a series of fan lobes on the basin floor. These lobes appear to be sourced from the north- northwest, indicating an affinity with the Bengal Fan. The lobes show an east-west avulsion pattern along the flank and crest of the present-day Shwe anticline. Only one of the four lobes is gas bearing and it is believed that this lobe was stratigraphically trapped by the incision of a younger gorge (blue gorge, Figure 15).

The upper reservoir series, the G3.2, was deposited at or near the toe of slope where the depositional pattern will change from Type A turbidites to Type C turbidites (Dattilo, 2013). Turbidites deposited in this region will consist of channel-levee complexes, crevasse splays, and incised gorges. There are numerous G3.2 series sands observed in the Shwe Field. It was not possible to correlate sands from well to well in such a manner as to keep the distribution of wet and pay sands geologically consistent. The G3.2A reservoir is interpreted as a gorge-fill sequence, which incised into the G5.2 reservoir series. The G3.2A reservoir is gas bearing and is likely stratigraphically trapped by a younger gorge sequence (blue gorge, Figure 15).

Slumps are common in turbidite depositional environments and one is observed removing the reservoir sands from well Shwe 1 (Figure 12 and Figure 14). It is possible that additional slump and debris flow deposits occur in the Shwe Field, particularly in the G3.2 series although the data available for this study is insufficient to determine whether these mass wasting deposits occur in the field. For simplicity, the G3.2 series were interpreted as multiple channels associated with the bypass facies of the Bengal Fan. Gas-bearing channels are oriented in such a manner

as to be stratigraphically trapped whereas those channels that are wet are oriented in such a way as to allow migration of gas out of the reservoir.

Acknowledgements

The authors thank Andy Racey for his thorough review of this paper.

References Cited

Baltar, D., and F. Roth, 2013, Reserves estimation methods for prospect evaluation with 3D CSEM data: First Break, v. 31/6, p. 103–110.

Beaubouef, R.T., 2004, Deep-water leveed-channel complexes of the Cerro Toro Formation, Upper Cretaceous, southern Chile: AAPG Bulletin, v. 88/11, p. 1471-1500.

Carter, P., 2015, Exploration Potential of the Rakhine Basin/Bengal Fan, Myanmar: SEAPEX Exploration Conference 2015, SEAPEX, Singapore, Web Accessed September 3, 2017, http://archives.datapages.com/data/southeast-asia-petroleum-exploration-society/data/027/027001/1_seapex0270005.htm

Clemenceau, G. R., J. Colbert, and D. Edens, 2000, Production Results from Levee-Overbank Turbidite Sands at Ram/Powell Field, Deepwater Gulf of Mexico: GCSSEPM Foundation 20th Annual Research Conference, Deep-Water Reservoirs of the World, December 3–6, 2000, Web Accessed September 3, 2017, http://gcsproceedings.sepmonline.org/content/gcs015/1/SEC11.body.pdf

Cliff, D., and P. Carter, 2016, Exploration of the Rakhine Basin, Pushing Out the Barriers with New 3D: Search and Discovery Article #10848, Web Accessed September 3, 2017, http://www.searchanddiscovery.com/documents/2016/10848cliff/ndx_cliff.pdf

Cossey, S., D. Kim, S.-Y. Yang, and H.Y. Jung, 2013, Identification and Implication of Injectites in the Shwe Gas Field, Offshore Northwestern Myanmar: Search and Discovery Article #20225., Web Accessed September 3, 2017, http://www.searchanddiscovery.com/documents/2013/20225cossey/ndx_cossey.pdf

Cross, N.E. A. Cunningham, R.J. Cook, A. Taha, E. Esmaie, and N. El Swidan, 2009, Three-dimensional seismic geomorphology of a deep-water slope-channel system: The Sequoia field, offshore west Nile Delta, Egypt: AAPG Bulletin, v. 93/8, p. 1063–1086.

Das, S., Y. Sastry, S. Mohan, and S.V. Rau, 2008, Biogenic Petroleum System of India's East Coast Deep Water Basins: 7th International Conference and Exposition on Petroleum Geophysics, Paper 374, Society of Petroleum Geophysicists, India, Web Accessed September 23, 2017, http://www.spgindia.org/2008/374.pdf

Dattilo, P., 2013, Basin Scale Typing of Deepwater Sediments: AAPG Search and Discovery Article #10484, Web Accessed September 23, 2017, http://www.searchanddiscovery.com/documents/2013/10484dattilo/ndx_dattilo.pdf

Filipov, A., R. Dilindi, and M. Drage, 2014, Electro-Magnetic Sensitivity in the Bengal Basin: Implications for Exploration in Myanmar, Bangladesh and NE India: International Petroleum Technology Conference, 10-12 December, Kuala Lumpur, Malaysia, Web Accessed September 23, 2017, https://www.onepetro.org/conference-paper/IPTC-17848-MS

Haughton, P., C. Davis, and W. McCaffrey, 2006, Facies Prediction in turbidite Fan Systems – Nature and Significance of 'Linked Debrites' in Sand-Rich Versus Mixed Sand-Mud Systems: Recent Advances in Siliciclastic Facies Models: Implications for Reservoir Characterization II (SEPM), AAPG Annual Convention, April 9-12, 2006 Technical Program, Web Accessed September 23, 2017, http://www.sepmstrata.org/page.aspx?pageid=37

Khonde, K., and R. Rastogi, 2013, Recent Developments in Spectral Decomposition of Seismic Data (Techniques and Applications): A Review, 10th Biennial International Conference and Exhibition, paper 28, Society of Petroleum Geophysicists, India, Web Accessed September 23, 2017, http://spgindia.org/10_biennial_form/P028.pdf

Kim, D., S.-Y. Yang, and J. Kim, 2012, Geological Modeling with Seismic Inversion for Deepwater Turbidite Fields Offshore Northwestern Myanmar: Search and Discovery Article #40877, Web Accessed September 3, 2017, http://www.searchanddiscovery.com/documents/2012/40877kim/ndx_kim.pdf

Kneller, B.C., 2012, Submarine Levees: Form, Process and Reservoir Prediction: Search and Discovery Article #50707, Web Accessed September 3, 2017, http://www.searchanddiscovery.com/documents/2012/50707kneller/ndx_kneller.pdf

Kneller, B., M. Dykstra, L. Fairweather, and J.P. Milana, 2016, Mass-transport and slope accommodation: Implications for turbidite sandstone reservoirs: AAPG Bulletin, v. 100/2, p. 213–235.

Lazarus, E.D., and J.A. Constantine, 2013, Generic theory for channel sinuosity: Proceedings of the National Academy of Sciences, v. 110/21, p. 8447-8452, Web Accessed September 22, 2017, http://www.pnas.org/content/110/21/8447.full.pdf

Mann, S., M. Lim, Q. Van De Laarschot, M. Keym, A. Jones, and R. Nesbit, 2017, Hydrate observations in the deepwater Rakhine Basin, Myanmar, Proceedings of the Third AAPG/EAGE/MGS Myanmar Oil and Gas Conference, Yangon Myanmar.

Nelson, H., H. Olson and J.E. Damuth, 2009, Modern Turbidite Depositional Patterns as Analogues for Subsurface Petroleum Plays in the Northern Gulf of Mexico: Search and Discovery Article #50214, Web Accessed September 22, 2017, http://www.searchanddiscovery.com/documents/2009/50214nelson/presentation.pdf

Pedersen, H.T., and M. Hiner, 2014A, Channel play in Foz do Amazonas – exploration and reserve estimate using regional 3D CSEM: First Break, v. 32/4, p. 95-100.

Pedersen, H.T., and M. Hiner, 2014B, Exploring channel reservoirs in a frontier area with regional CSEM as fluid indicator: 2014 SEG Annual Meeting, 26-31 October, Denver, Colorado, USA, Web Accessed September 22, 2017, https://www.onepetro.org/conference-paper/SEG-2014-0825

Prather, B.E., 2003, Controls on reservoir distribution, architecture and stratigraphic trapping in slope settings: Marine and Petroleum Geology, v. 20, p. 529-545, Web Accessed September 22, 2017, https://www.researchgate.net/publication/222509254_Controls_on_reservoir_distribution_architecture_and_stratigraphic_trapping_in_slope_settings

Prather, B.E., 2016, The Practice of Seismic Stratigraphy in Deepwater Settings: geoLogic News, 2nd Edition, Subsurface Consultants & Associates, LLC, Houston. https://www.scacompanies.com/wp-content/uploads/2016/07/GeoLOGIC-2016-2.pdf

Sawyer, D.E., P. B. Flemings, R. C. Shipp, and C.D. Winker, 2007, Seismic geomorphology, lithology, and evolution of the late Pleistocene Mars-Ursa turbidite region, Mississippi Canyon area, northern Gulf of Mexico: AAPG Bulletin, v. 91/2, p. 215–234.

Shipp, R.C., R.C. Shoup, and F.A. Diegel, 2000, High-Resolution Near-Surface Seismic Analogs for Deep Subsurface Canyon/Channel-Margin Slides, AAPG Hedberg Research Conference, "Integration of Geologic Models for Understanding Risk in the Gulf of Mexico," September 20–24, 1998, Web Accessed September 22, 2017, http://archives.datapages.com/data/specpubs/discovery1/D0117/IMAGES/2_07.pdf

Subrahmanyam, D., and P.H. Rao, 2008, Seismic Attributes - A Review: 7th International Conference & Exposition on Petroleum Geophysics, Hyderabad 2008, paper 398, Society of Petroleum Geophysicists, India, Web Accessed September 22, 2017, https://www.spgindia.org/2008/398.pdf

Yang, S.-Y., and J.W. Kim, 2014, Pliocene basin-floor fan sedimentation in the Bay of Bengal (offshore northwest Myanmar): Marine and Petroleum Geology, v. 49, p. 45-48, Web Accessed September 3, 2017, http://www.sciencedirect.com/science/article/pii/S0264817213002390

Yang, S.-Y., C. Lee, and H. Yi, 2015, Shwe Gas Field: Discovery to Production Rakhine Basin, Offshore Northwest Myanmar: SEAPEX Exploration Conference 2015, SEAPEX, Singapore.

Yi, H., C. Lee, and D.-Y. Kim, 2015, Shwe Ga Development, Rakhine Offshore, Myanmar: SEAPEX Exploration Conference 2015, SEAPEX, Singapore, Web Accessed September 3, 2017, http://archives.datapages.com/data/southeast-asia-petroleum-exploration-society/data/027/027001/1_seapex0270006.htm

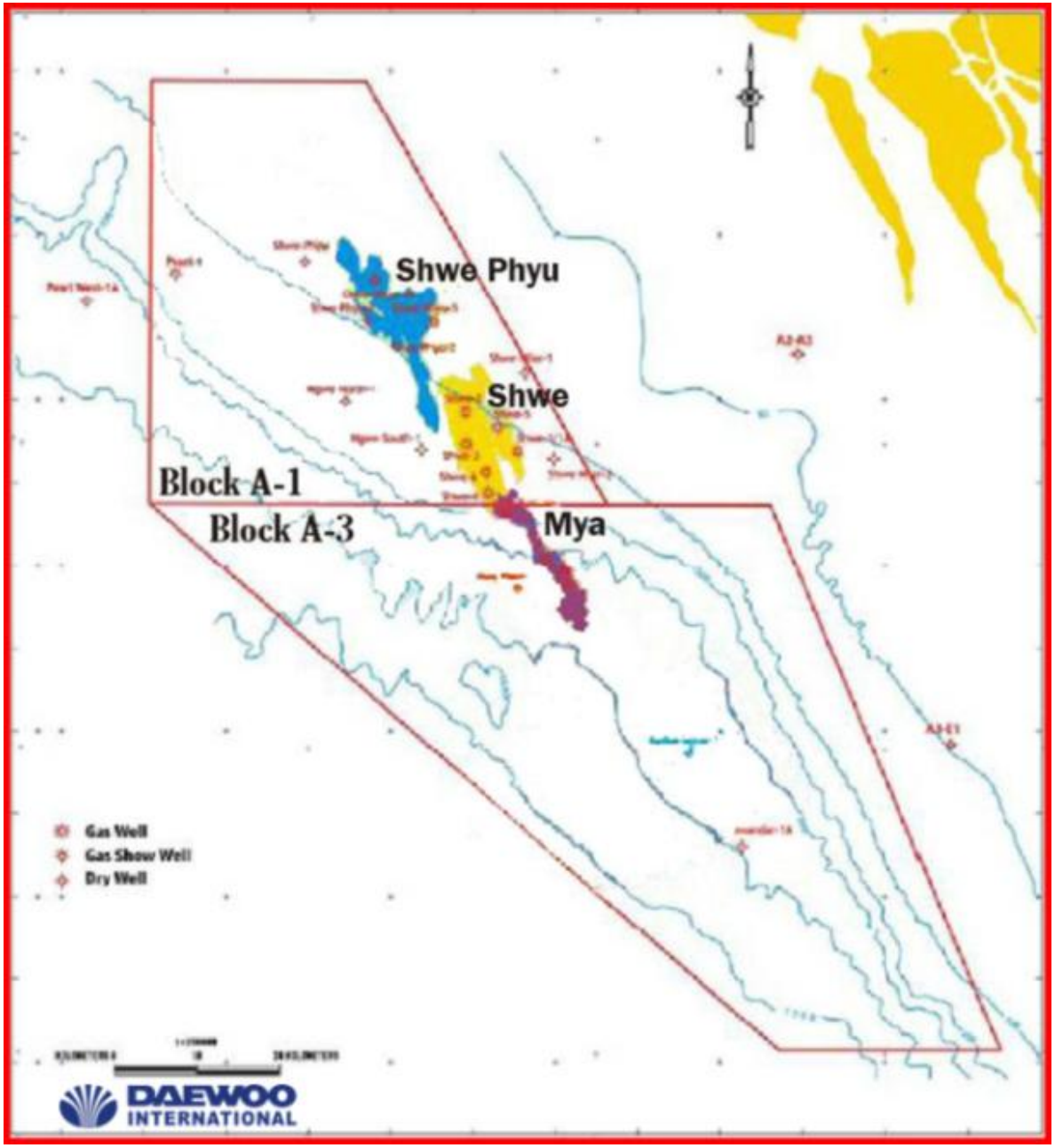

Figure 1. Location Map, Shwe, Shwe Field offshore Myanmar (Yi, et al, 2015).

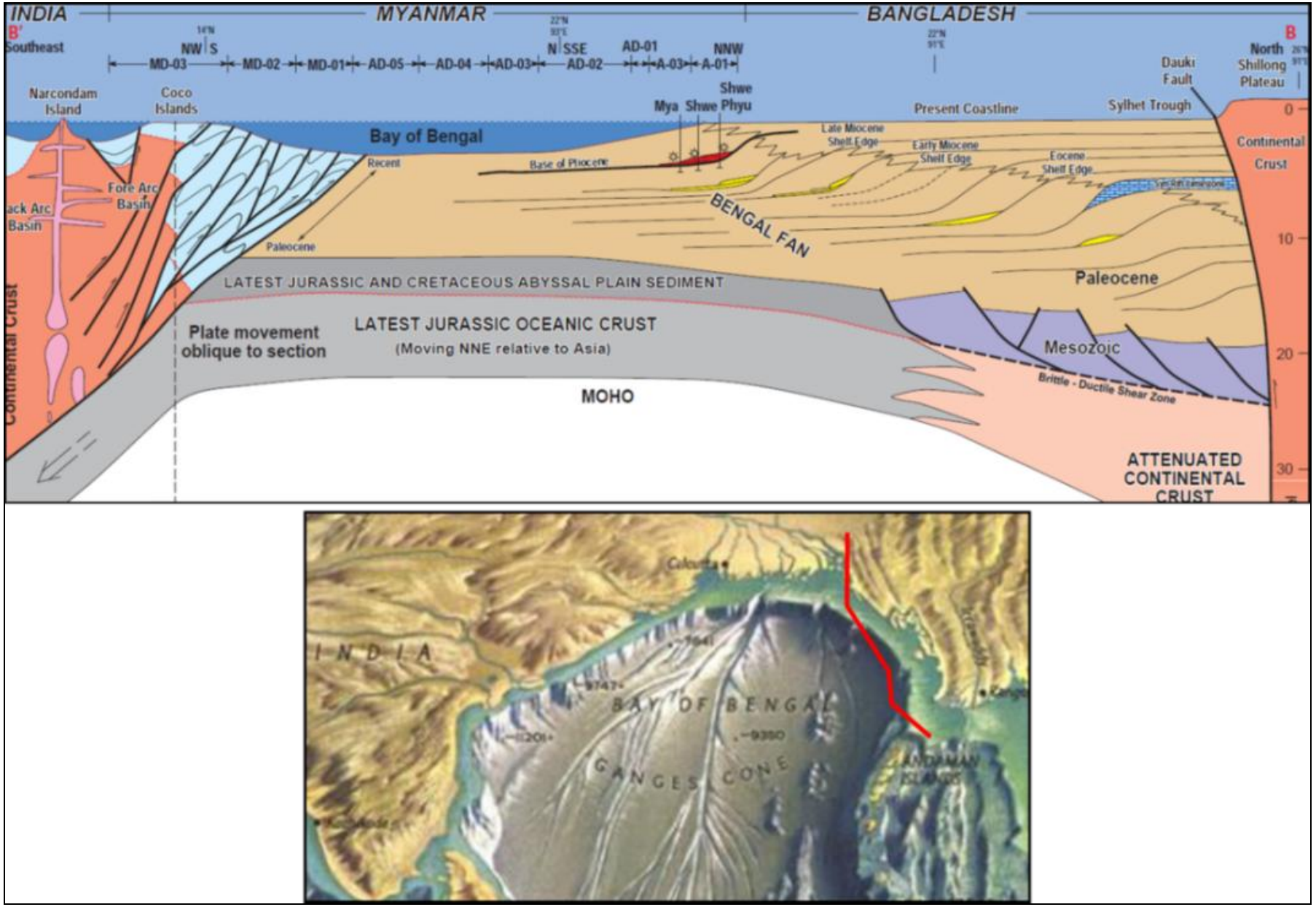

Figure 2. Depositional setting of the Shwe, Shwe Phyu, and Mya Fields (after Carter, 2015).

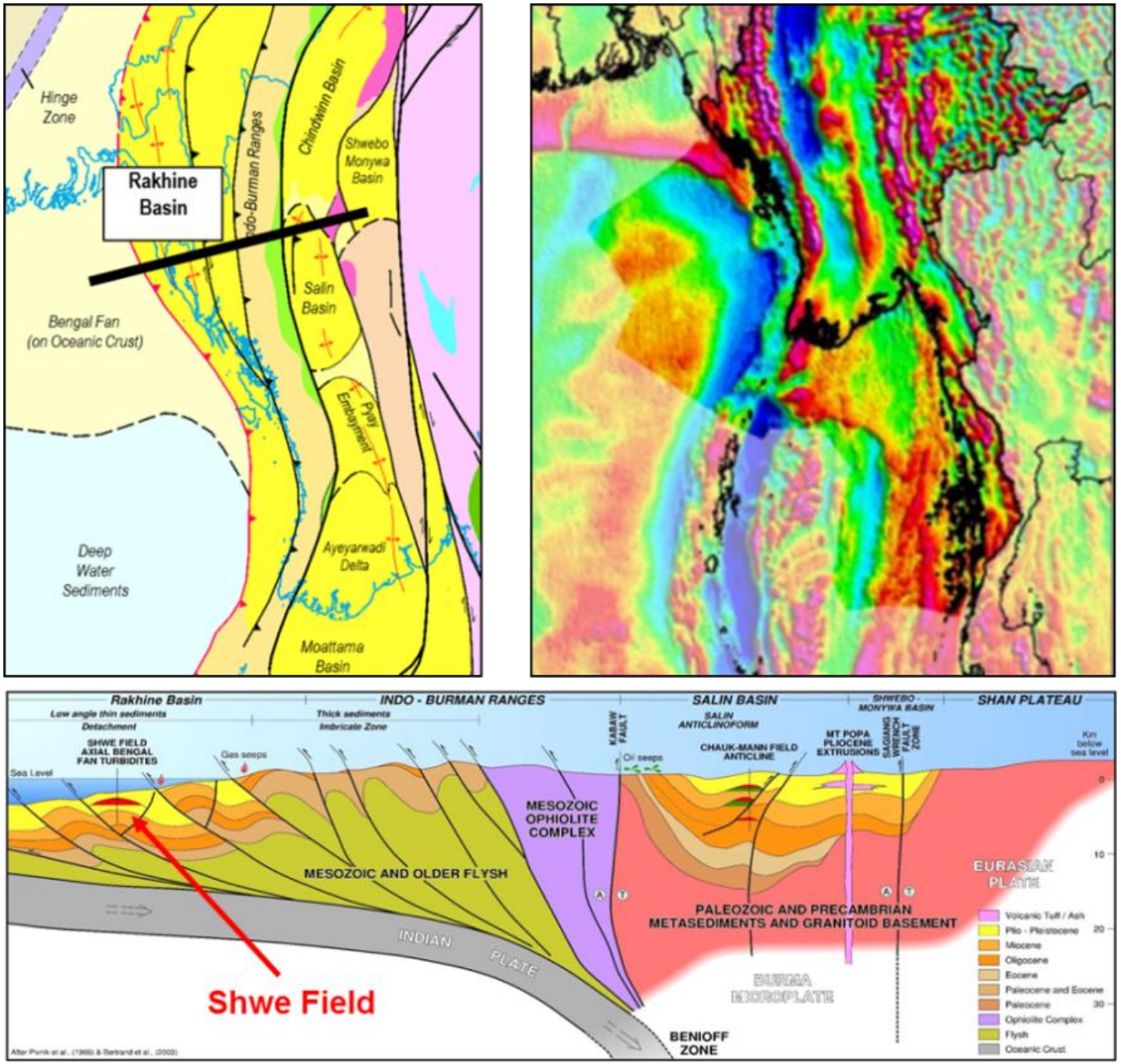

Figure 3. Rakhine Basin, Myanmar (from Cliff and Carter, 2016).

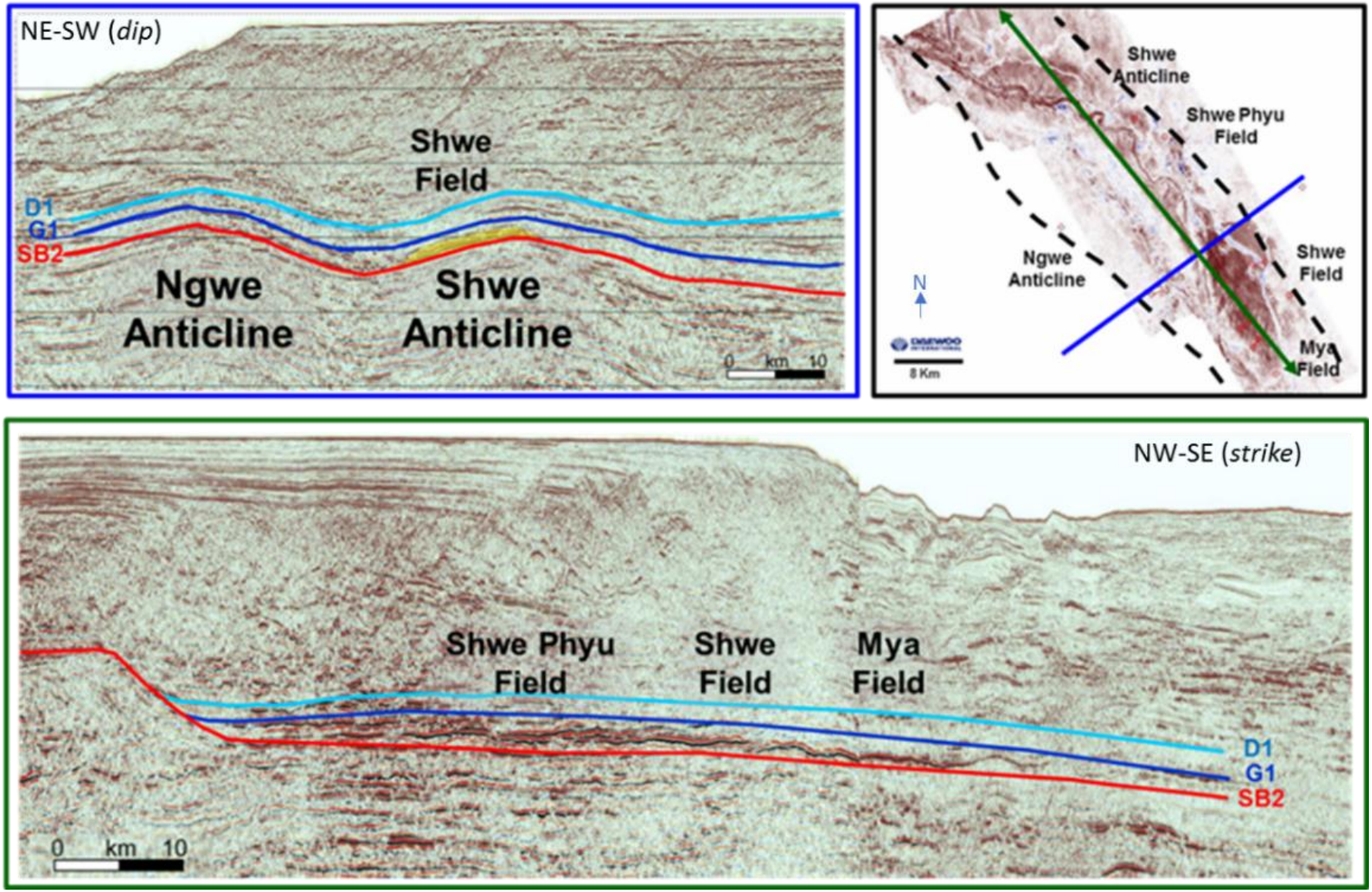

Figure 4. Strike and dip profiles across Shwe (correlations and map from Yang and Kim, 2014).

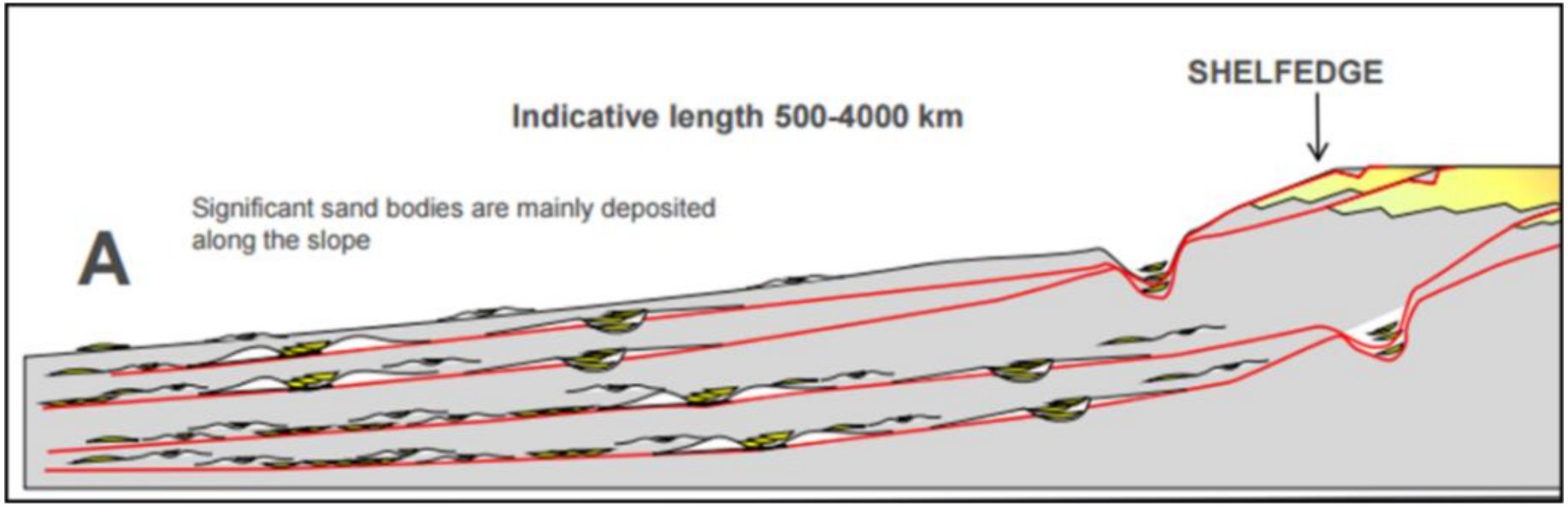

Figure 5. Type A Turbidite System deposited on unconstrained slopes (from Dattilo, 2013).

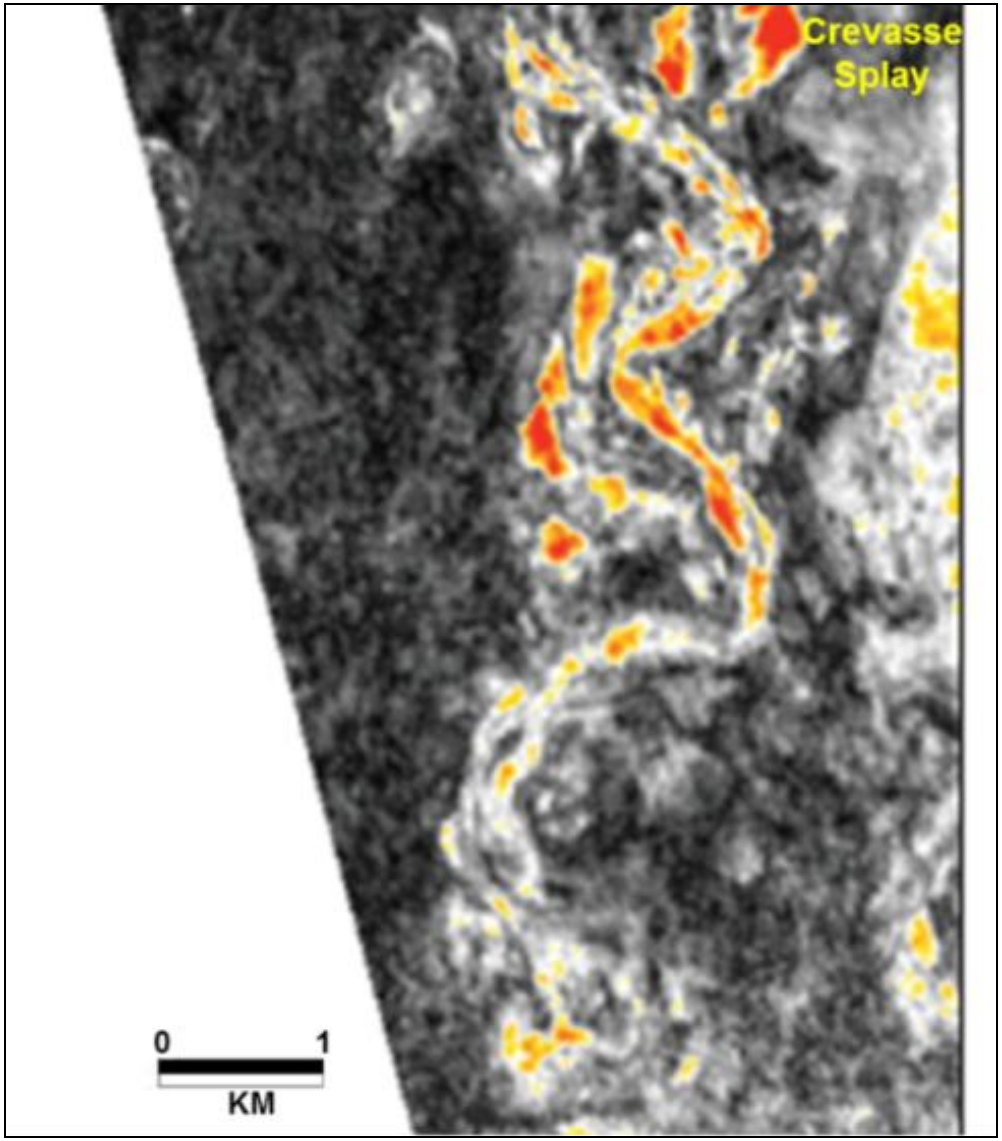

Figure 6. Unconstrained slope deposits, Sequia Field, offshore Egypt (from Cross et al, 2009).

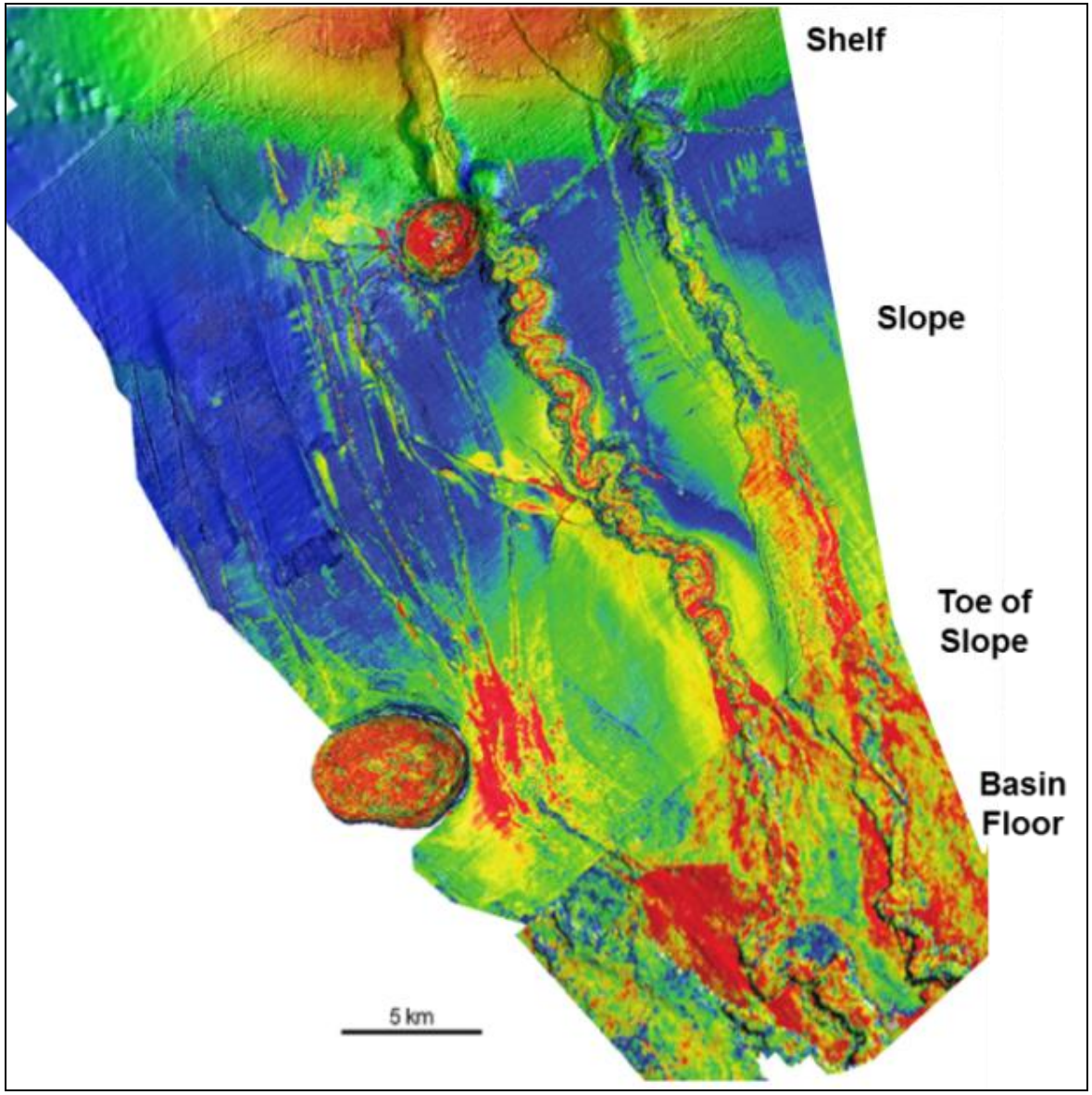

Figure 7. Lobate fan deposition occurs on the basin floor near the toe of slope as seen in this example from the northeast Gulf of Mexico (Prather, 2016).

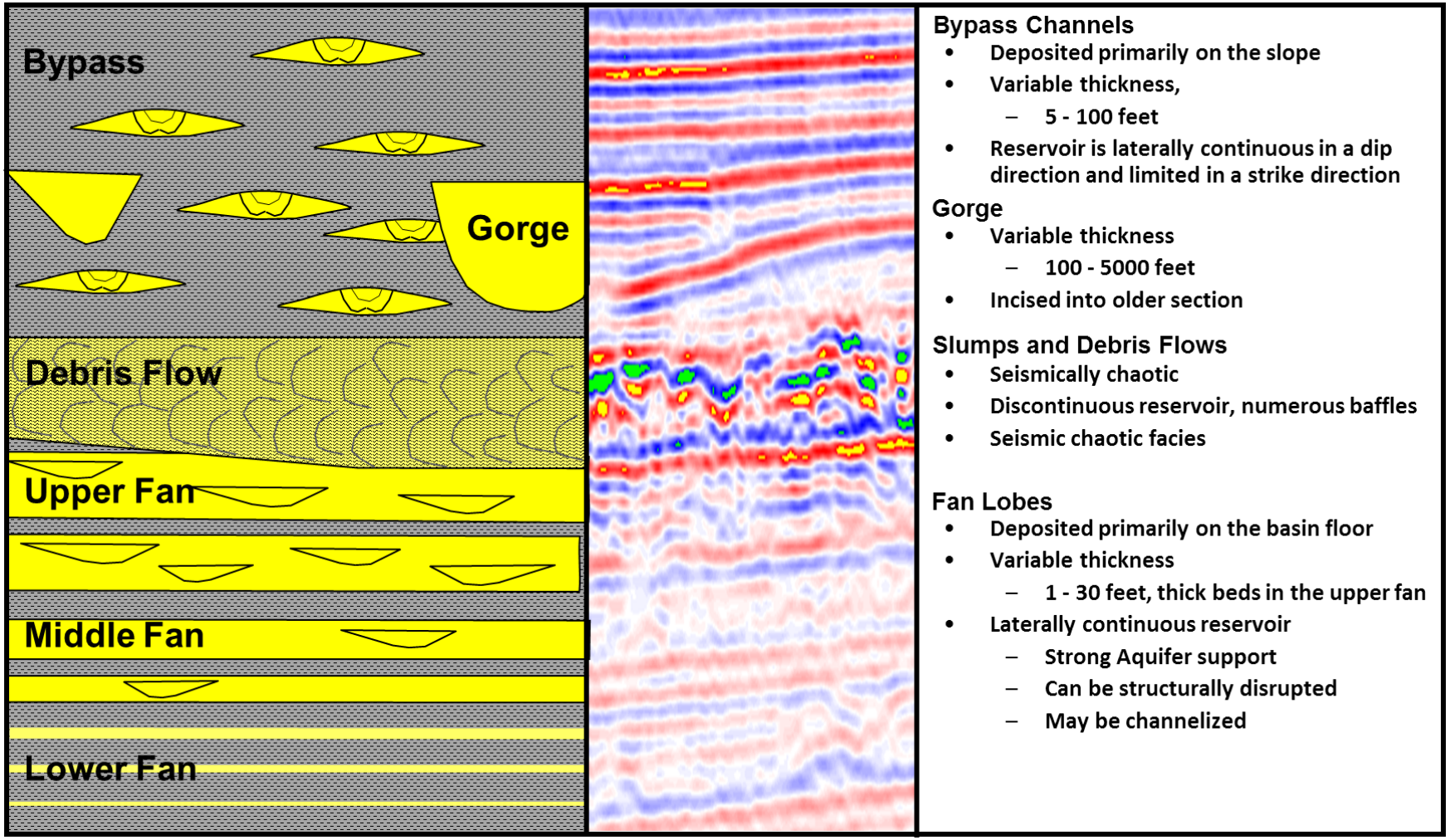

Figure 8. Deepwater depositional facies.

Figure 9. Soft sediment deformation in a turbidite bed, Myanmar. Bed is ~ 1 meter thick.

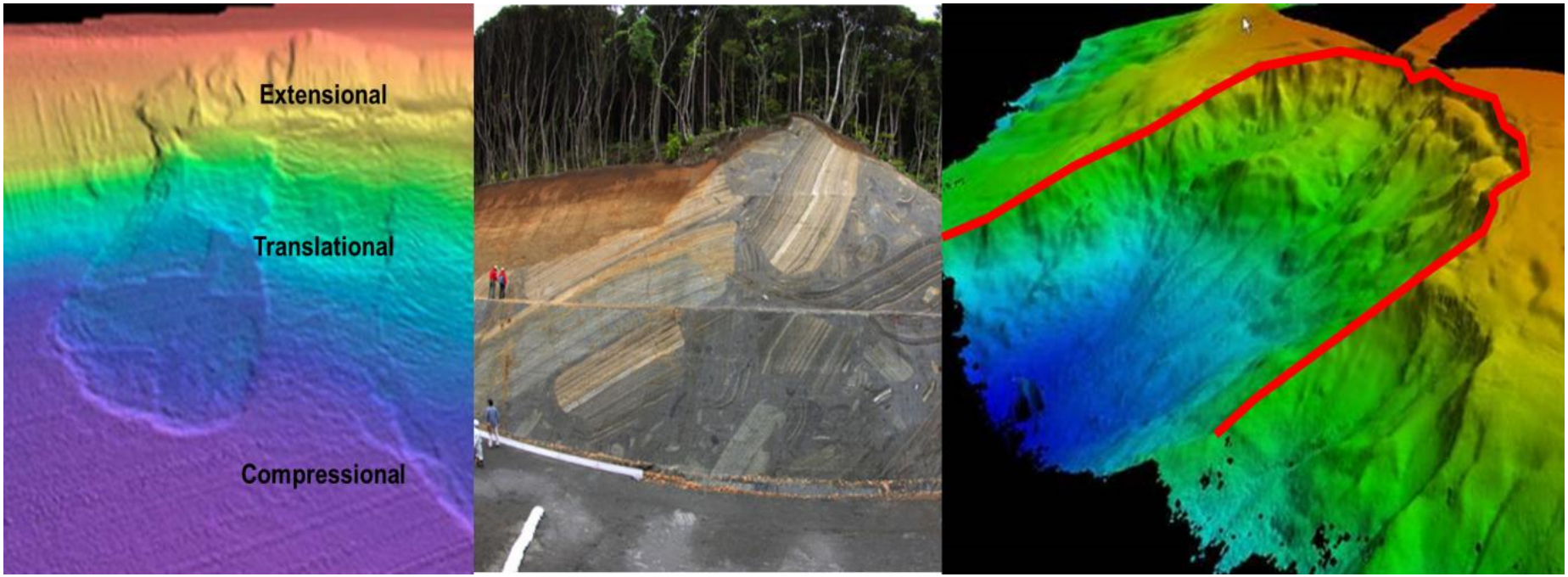

Figure 10. Various examples of Debris Flows (left and center) and a slump (right).

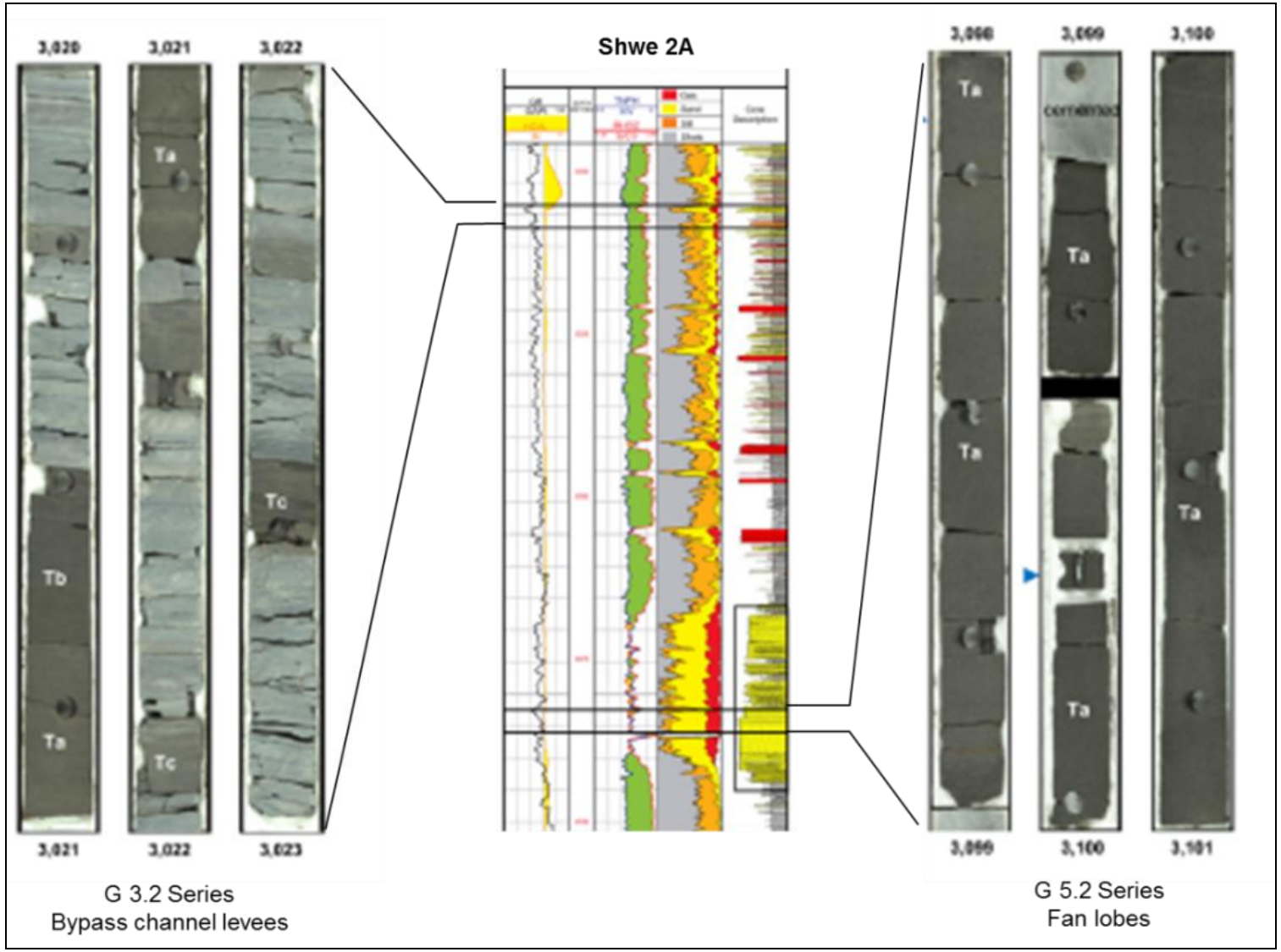

Figure 11. Core photos for the G3.2 (left) and G5.2 reservoirs (right), Shwe 2A (Yang and Kim, 2014).

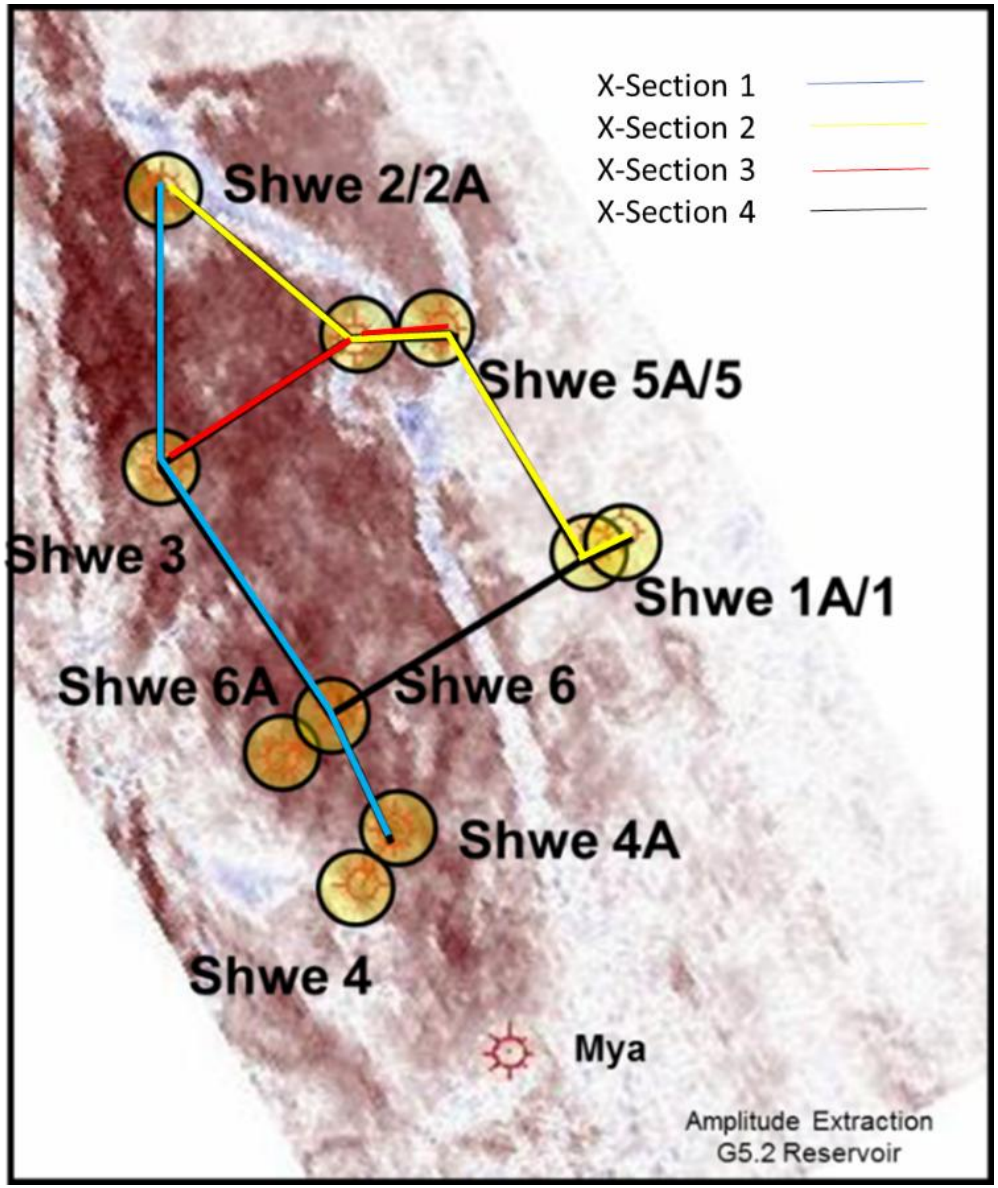

Figure 12. Cross section (G5.2 seismic amplitude map from Cossey et al. 2013).

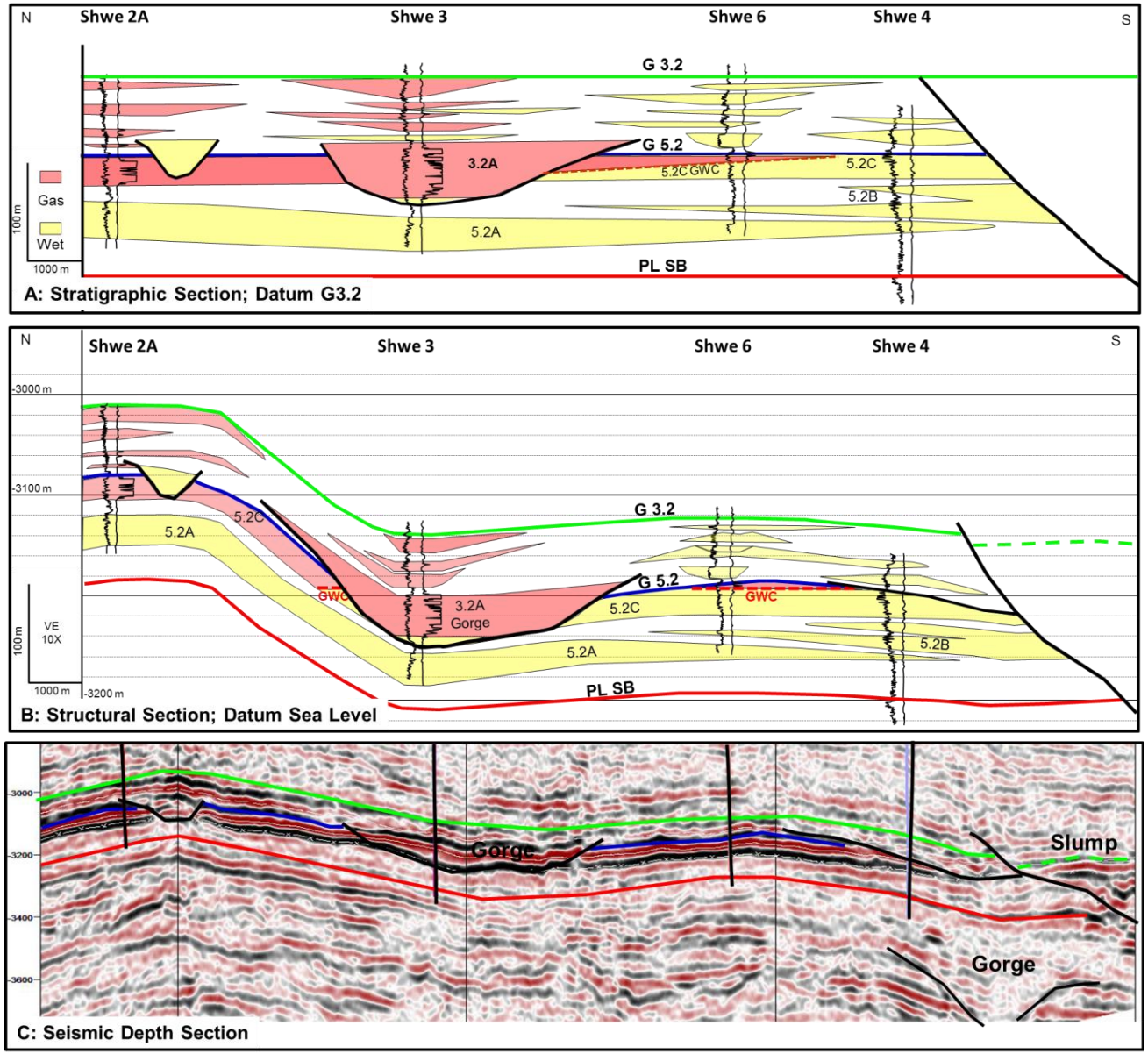

Figure 13. Cross section 1, Shwe Field (Location shown in Figure 12).

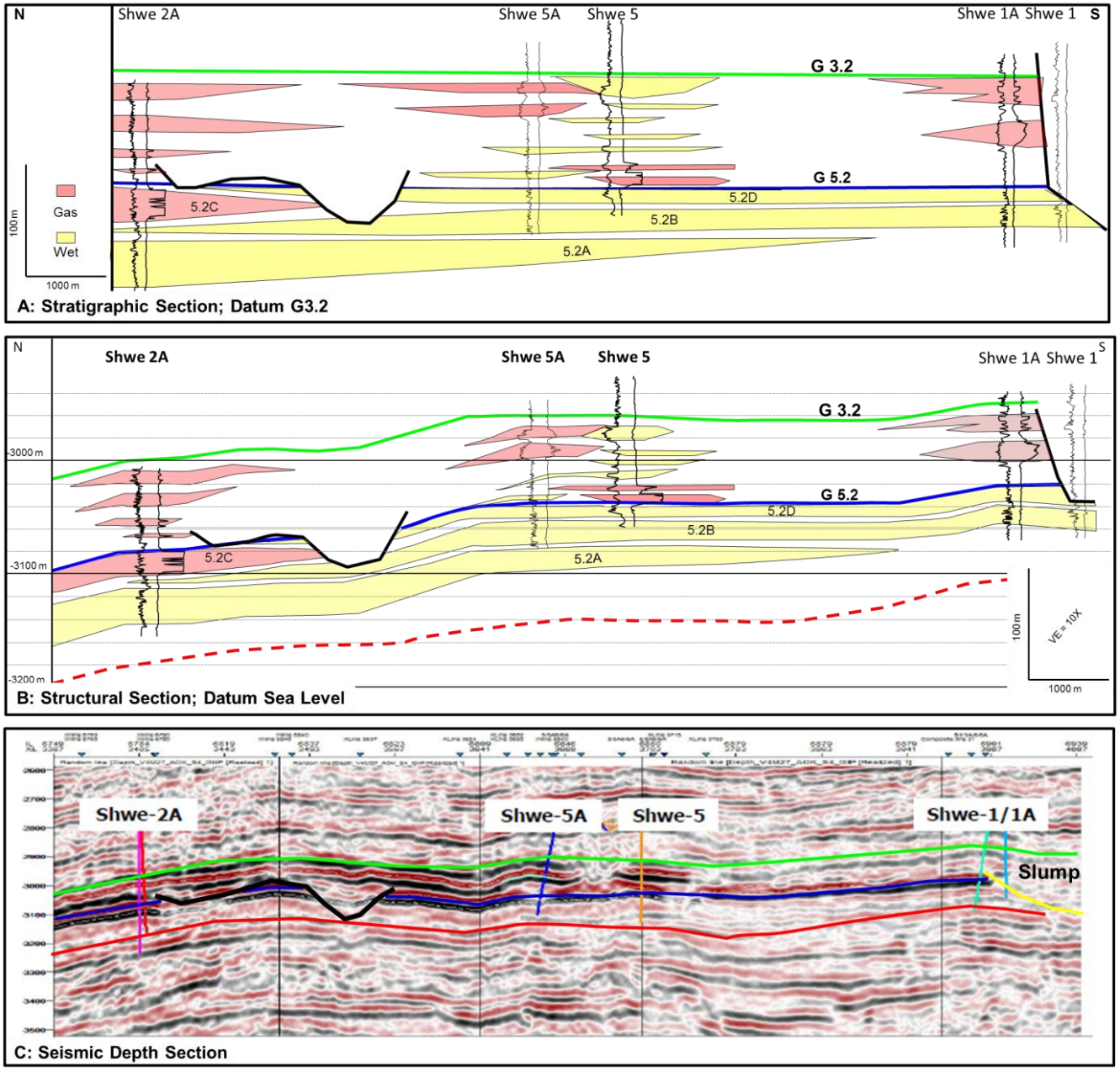

Figure 14. Cross section 2, Shwe Field.

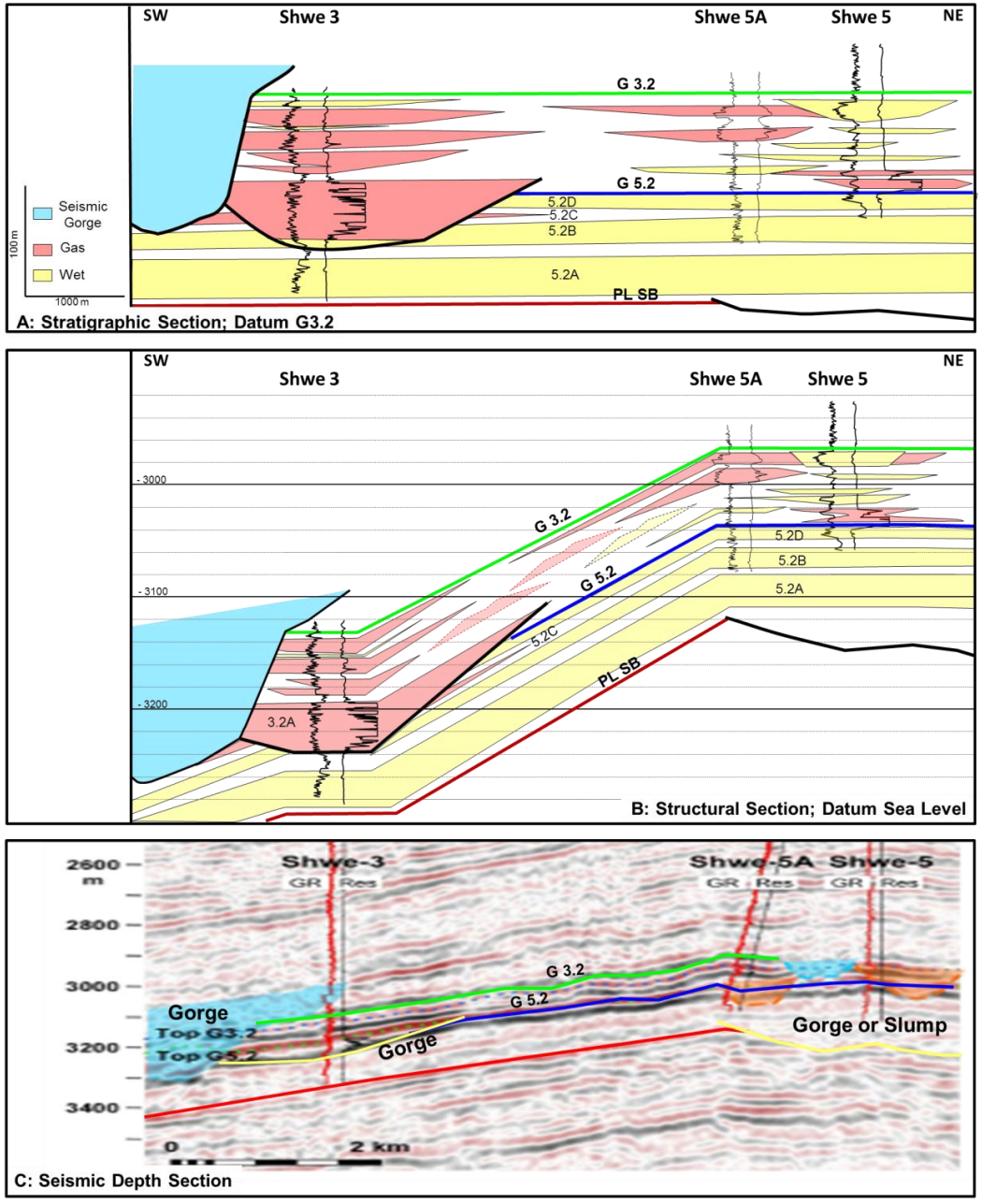

Figure 15. Cross section 3, Shwe Field.

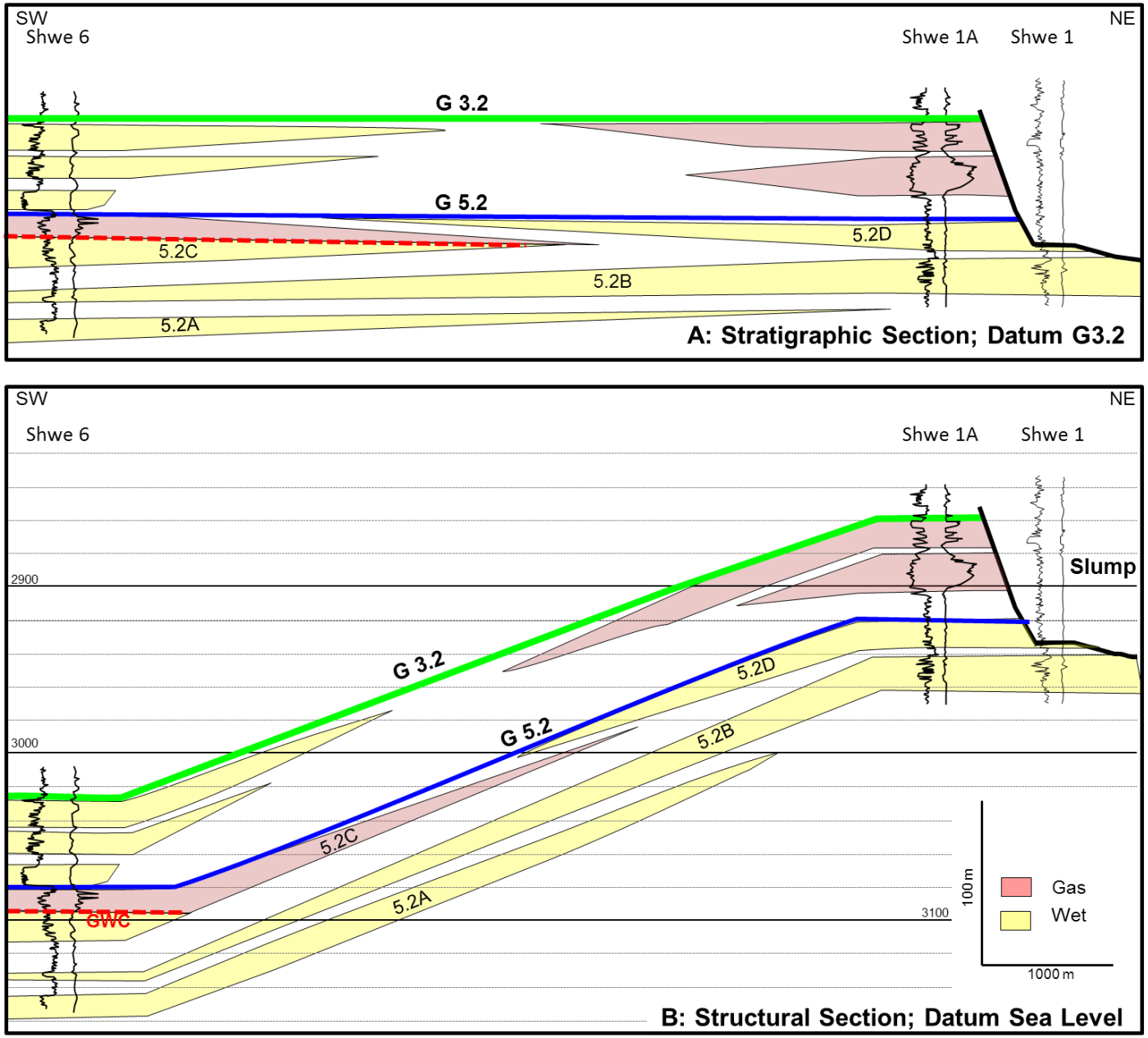

Figure 16. Cross section 4, Shwe Field.

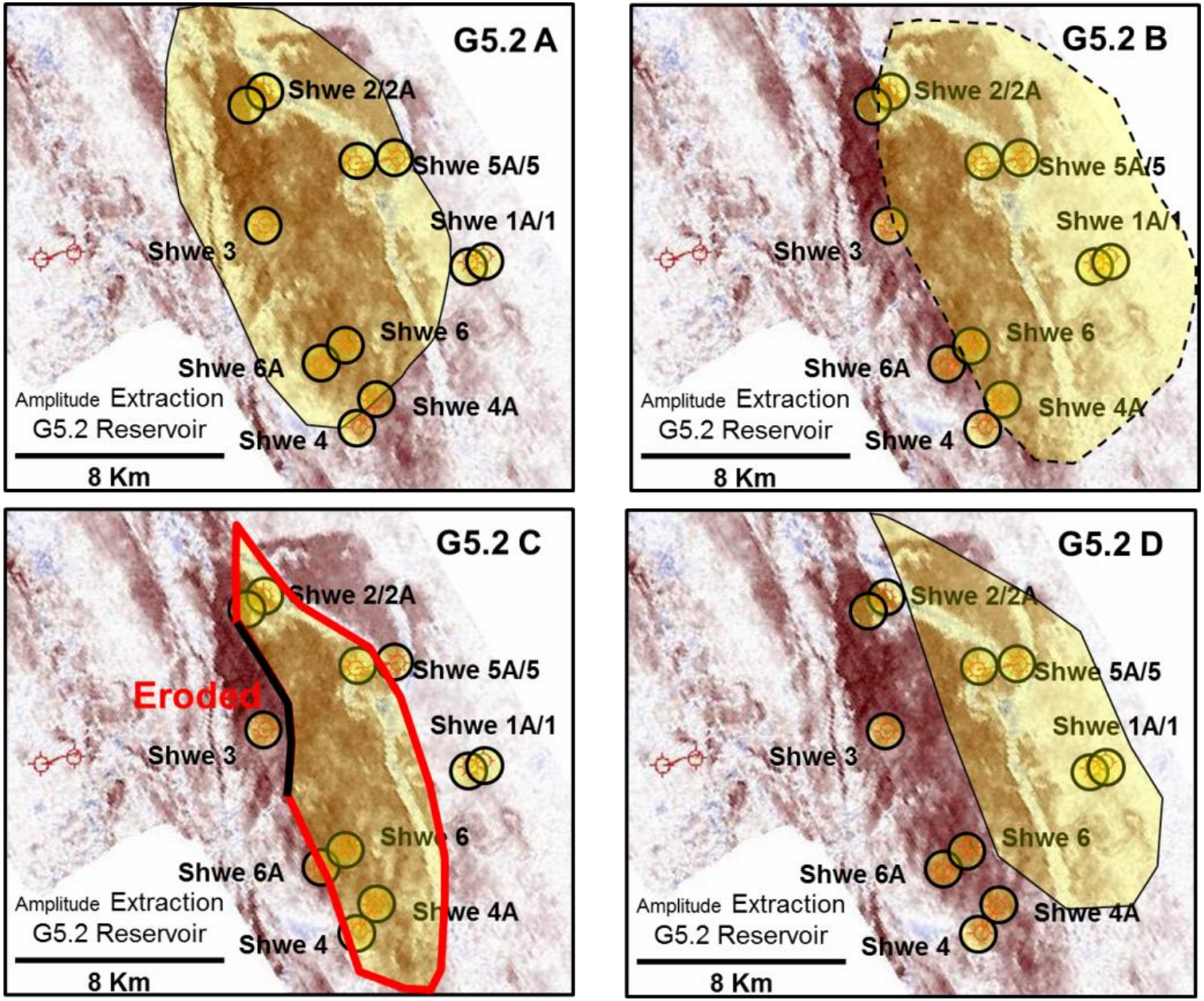

Figure 17. Depositional interpretation for the G5.2A – D fan lobes.

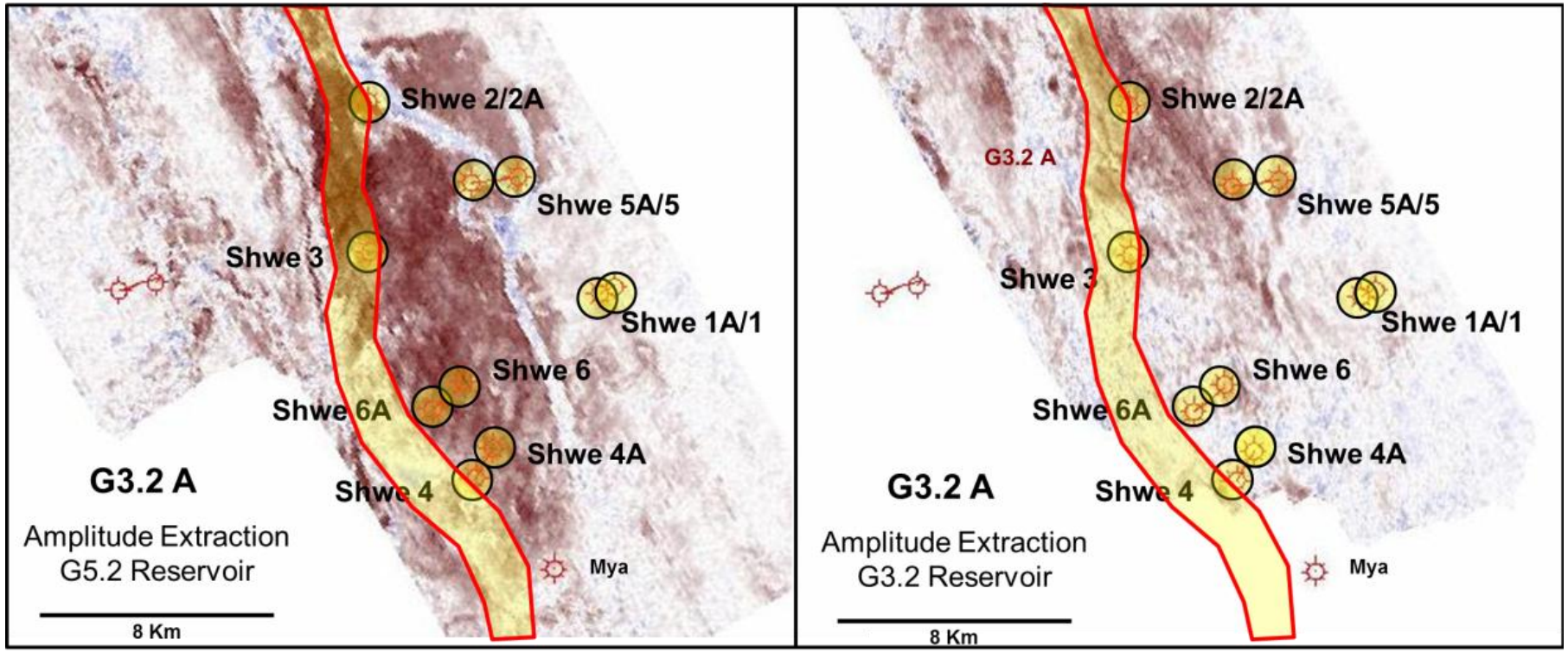

Figure 18. Depositional interpretation for the G3.2A gorge.

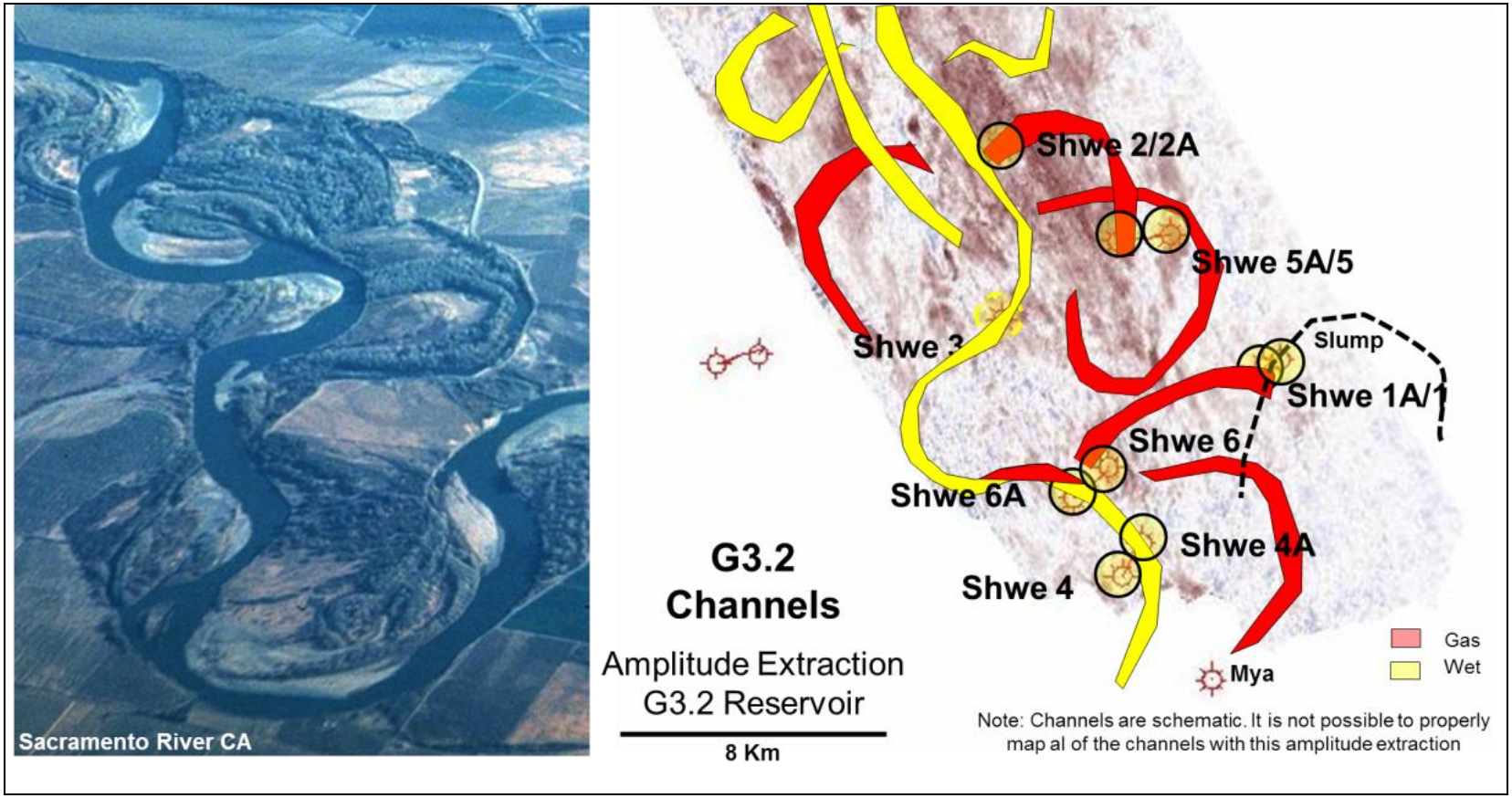

Figure 19. Depositional interpretation for the G3.2 bypass channels with analogue.

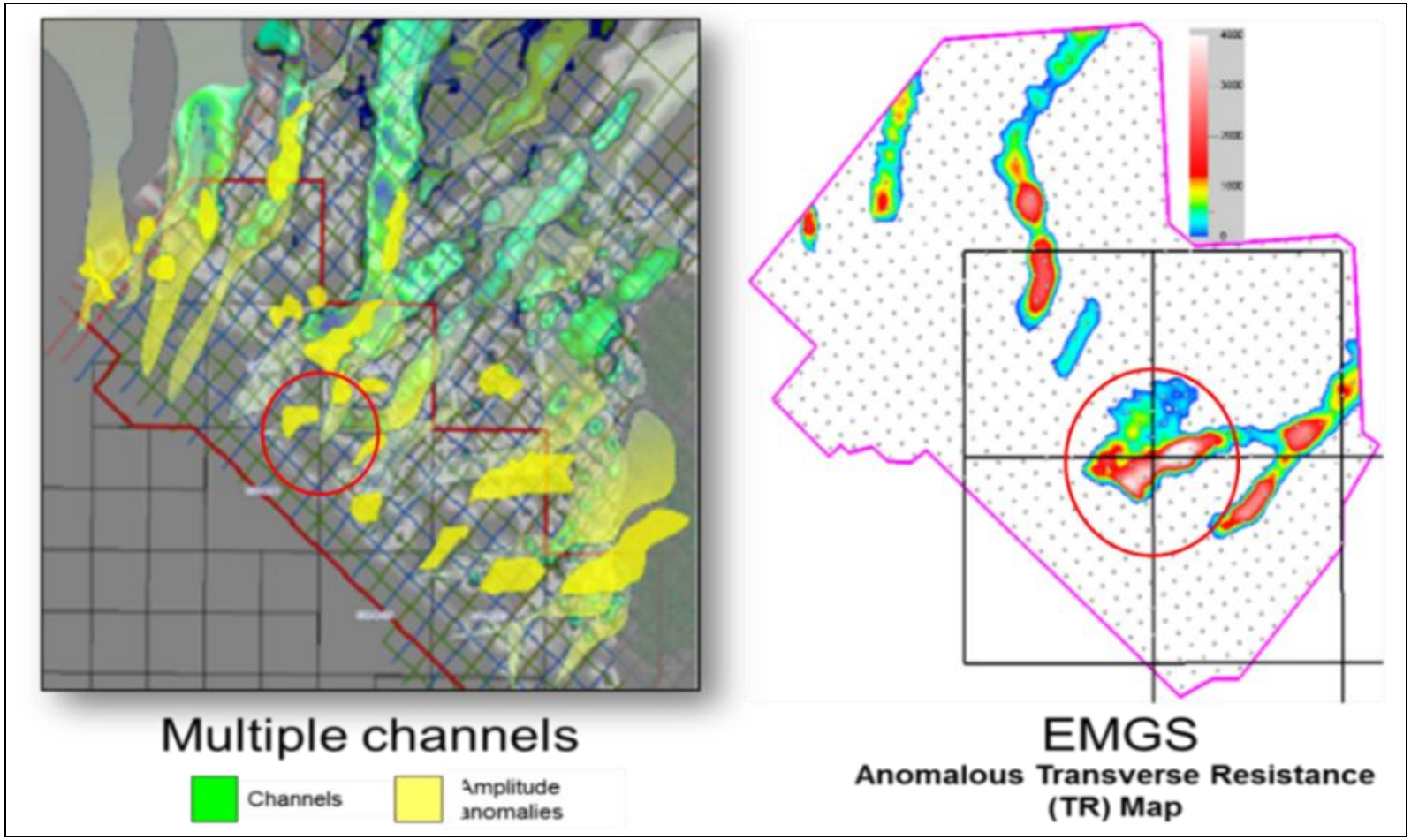

Figure 20. 2D Seismic data amplitude extraction map and a corresponding CSEM survey Foz do Amazonas Basin, Brazil (Courtesy of EMGS).

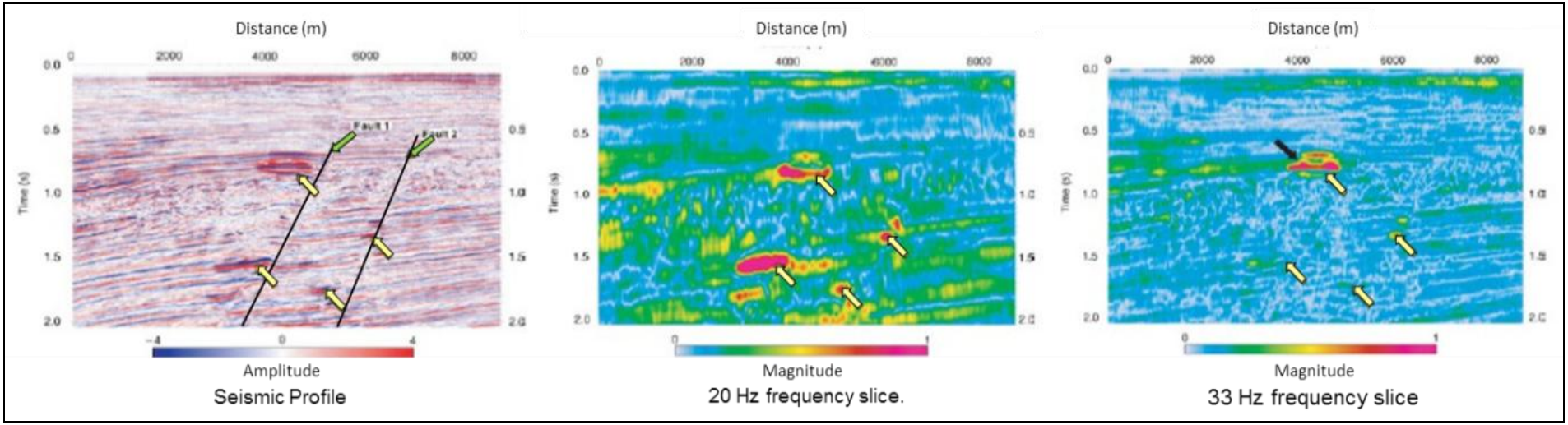

Figure 21. Application of spectral decomposition to differentiate hydrocarbons. Modified from Khonde and Rastogi (2013).